4-4-2017

Evaluating the impact of different types of stabilized bases on the overall performance of flexible pavements

Andrae Anthony Francois
Rowan University

EVALUATING THE IMPACT OF DIFFERENT TYPES OF STABILIZED BASES ON THE OVERALL PERFORMANCE OF FLEXIBLE PAVEMENTS

by

Andraé Anthony François

A Thesis

Submitted to the
Department of Civil and Environmental Engineering
College of Engineering
In partial fulfillment of the requirement
For the degree of
Master of Science in Civil Engineering
at
Rowan University
November 21, 2016

Thesis Chair: Yusuf Mehta, Ph.D.

Dedications

I would like to dedicate this document to my parents, Gary François and Marilyn Thomas-François as well as my sister, Marisa Adele-Marie Gray, for their continuous support of all my academic endeavors.

Acknowledgements

I would like to express my heartfelt gratitude to Professor Dr. Yusuf Mehta who has guided me during my research and provided sound academic advice throughout my graduate career thus far. I will also like to thank Dr. Ayman Ali and Dr. Hashim Rizvi who have also advised and assisted me throughout my research. Lastly, I would like to acknowledge my aunts, Maria D. Thomas and Beverly A. Thomas for the assistance they provided in editing this document.

Abstract

Andraé François
EVALUATING THE IMPACT OF DIFFERENT TYPES OF STABILIZED BASES ON THE OVERALL PERFORMANCE OF FLEXIBLE PAVEMENTS
2016-2017
Yusuf Mehta, Ph.D.
Master of Science in Civil Engineering

This study was initiated with the aim of evaluating the impact of stabilized and untreated base layers on the performance (i.e., fatigue and rutting) of flexible pavements. Four field sections constructed using stabilized base layers (i.e., bituminous (asphalt emulsion), calcium chloride ($CaCl_2$), Portland cement, and geogrid stabilized base layers) and a control section constructed using untreated RAP aggregates were analyzed in this study. Falling Weight Deflectometer (FWD) tests were conducted on all the field sections and the collected data was used to backcalculate the elastic moduli for all layers. The influence of the stabilized bases and the untreated RAP base on the mechanical responses (stresses and strains) of the overall pavement structure was also evaluated by conducting layered elastic analyses. Pavement ME simulations were also conducted to determine which of the four stabilized bases enhanced the predicted performance of flexible pavements the most. Based on the results of the study, it was concluded that the Portland cement stabilized base seemed to be more effective than the other stabilized bases at improving the resistance of the pavement sections to fatigue cracking. It was also determined that base layer stabilization appeared to have little effect on the rutting resistance of the pavement sections.

Table of Contents

Table of Contents (Continued)

Table of Contents (Continued)

List of Figures

List of Tables

Chapter 1

Introduction

Pavement performance is influenced by both the pavement structure and the properties of its respective layers. Structural failure in a pavement occurs when the mechanical responses, such as the horizontal tensile strains at the bottom of the surface layer and/or the vertical deformation in each of the layers exceed a criterion. The tensile strains and the deformation in these layers cause major distresses such as fatigue cracking and rutting to develop in flexible pavements. These distresses tend to reduce the ability of flexible pavements to withstand traffic loads because they decrease the overall structural capacity of the pavement structure. Pavement distresses like fatigue cracking and rutting also reduces the smoothness or "rideability" of a pavement surface and this in turn decreases the safety and quality of ride the pavement provides for road users.

In flexible pavements, tensile strains develop at the bottom of each layer when a traffic load is applied. However, the tensile strains that form at the bottom of the hot mix asphalt (HMA) layer are responsible for bottom-up fatigue distresses that arise in the wearing course of a flexible pavement. As the number of load repetitions due to traffic increases on a pavement structure, the horizontal tensile strain at the bottom of the HMA layer also increases. This causes micro-cracks to form at the bottom of the HMA layer. When the strain on the asphalt layer reaches the tensile limit or fatigue threshold of the HMA, these micro-cracks develop into macro-cracks. If the pavement continues to be subjected to repeated traffic loads, these macro-cracks then begin to propagate upward, until they become visible at the surface of the pavement. The formation and propagation

of macro-cracks in the HMA layer of flexible pavements hinders the ability of the layer to effectively distribute traffic loads to the underlying layer (i.e. the base layer) and allows increased moisture or runoff to enter the pavement structure. Therefore, the tensile strains which cause these macro-cracks to form, contribute to a reduction in the overall structural capacity of flexible pavements and negatively impact on pavement performance.

Pavement performance is also affected by the vertical stress at the top of the subgrade. Large vertical stress on the top of the subgrade causes detrimental permanent deformation to occur. The role of pavements is to limit the vertical stress on the subgrade. The resilient modulus of the subgrade determines the maximum vertical stress (i.e. allowable stress) the subgrade could withstand before it experiences significant deterioration. This relationship between the vertical compressive stress and the resilient modulus of the subgrade is quantified by the vertical compressive strains at the top of the subgrade [1]. If there are large vertical compressive strains at the top of the subgrade, the vertical stress on the subgrade due to traffic loads may exceed the resilient modulus of the subgrade. This may cause detrimental permanent deformation to occur within the pavement structure which in turn may lead to severe rutting (i.e. permanent deformation) in the flexible pavement. When there is severe rutting in a flexible pavement, depressions form at the surface of the pavement along the wheel path. These depressions reduce the serviceability of the flexible pavement and have a negative impact on the overall performance of the pavement.

Background

The stiffness of the base layer can significantly influence the tensile strains in the HMA layers and the compressive strains on the subgrade layer of flexible pavements. Since the stiffness of the base layer depends on the material properties of that layer, the type of base layer used in a flexible pavement can have an effect on the overall performance of flexible pavements. Generally, two types of base layers are utilized in the flexible pavements; unbound aggregate bases and bound (stabilized) aggregate bases. Unbound aggregate bases consist of untreated granular materials (e.g., naturally-existing, crushed aggregates) while stabilized bases consist of granular material bounded by a stabilizing agent (e.g., asphalt emulsion, foamed asphalt, or cement). The functions of all base layers, regardless of their type, are to provide support for the HMA layer(s) and to efficiently distribute traffic loads onto subgrade and/or subbase pavement layers.

Load transfer in both unbound and bound bases involves the transference of traffic-induced stresses along load carrying aggregate chains. The aggregate interlock between these aggregate chains (and the aggregates in a particular chain) facilitates load transfer and significantly influences the ability of base layers to withstand traffic loads. In unbound pavements, aggregate chains consist of continuous columns of aggregates which actually carry and transfer the load. These continuous columns of aggregates are laterally supported by the aggregates between individual aggregate chains that do not carry any load [2]. When a critical load (i.e., failure load) is applied to a base layer, load carrying chains fail; thus, forcing aggregate particles to realign to form new load carrying chains. This aggregate realignment process results in permanent deformation (or rutting) which in turn reduces both the structural capacity and stability of base layers. Studies have

shown that permanent deformation in unbound bases is directly related to the load transfer by the shear in the load carrying aggregate columns [2]. This implies that aggregate interlock influences the level of permanent deformation in unbound base layers and the overall flexible pavement structure.

Two types of stresses affect the performance of unbound (untreated) base layers when traffic loads are applied to flexible pavement. These stresses include the residual stresses due to compaction of the in-situ material (i.e. subbase and subgrade) and the vertical stresses due to moving traffic loads. The residual stresses in the granular layers of flexible pavements are static stresses that generally increase as depth from the surface increases. The vertical stresses under moving wheel loads create dynamic shear stresses between adjacent aggregates that are highest directly below the wheel load and decrease as radial distance from the moving wheel load increases [2]. The ability of the aggregates in unbound base layers to withstand the combination of these two types of stresses determines how an unbound base layer will perform. The impact of unbound base layers on overall pavement performance will therefore depend on the depth of the layer from the surface and the stiffness properties of the in-situ layers below.

The treatment of untreated granular aggregates with stabilizing agents provides bound bases with improved stability because stabilization increases aggregate interlock and facilitates load transfer. However the actual stabilizing agents themselves contribute very little to the structural capacity of the bound base. There is a variety of stabilizing agents currently used to treat the base layers of flexible pavements. Some of the commonly used stabilizers in bound bases include: foamed asphalt, cutback asphalt, Portland cement concrete (PCC), geogrids, and calcium chloride ($CaCl_2$). The increased

aggregate interlock provided by these stabilization agents enables load transfer in bound bases to be more efficient than the load transfer in unbound bases.

Problem Statement

There is a general consensus among researchers [3, 4, 5, 6, 7, 8, 9, 10] that the use of stabilizing agents in the base layer of flexible pavements improves the overall performance of that layer. However, there is limited insight on how different types of stabilized base layers compare in terms of their impact on the overall performance of flexible pavements. To better understand the impact of stabilized base layer stabilization on pavement performance there is a need to conduct a controlled study with pavement sections that contain different types of bounded base layers. These stabilized base layers should be constructed with the same thickness, similar aggregates, similar aggregate gradation, and similar material properties above and below the bound base, in order to capture the true effect of base layer stabilization on overall pavement performance.

Significance of Study

This study is designed to evaluate the impact of different types of stabilized base layers on the predicted performance of flexible pavements. Previous studies conducted on stabilized bases have evaluated how changes in the physical properties of the stabilized material have affected the overall laboratory performance of the base layer. However, this study will provide a direct comparison of how the changes in the mechanical responses of various types of stabilized base layers affect the overall performance of flexible pavements. Determining the best performing stabilizing agent and aggregate types will enable state transportation agencies (STAs) to make better informed decisions when

selecting base layers for future flexible pavement infrastructure. This will reduce overall pavement maintenance costs since transportation officials will be able to design flexible pavements that require less rehabilitation and maintenance throughout the pavement life.

Hypothesis

The fatigue (i.e. tensile strains below the HMA layer) and rutting (i.e. the compressive strains at the top of the subgrade) performance of flexible pavements that contain bound bases are more than likely influenced by the type of stabilizing agent used to treat the base layer.

Goal & Objectives

The main objective of this study is to evaluate the impact of stabilizing agent on the overall pavement performance. (i.e., bases stabilized using calcium chloride, emulsified asphalt, Portland cement, and geogrids) and one control base layer (untreated Reclaimed Asphalt Pavement (RAP) base) on the overall performance and life cycle costs of flexible pavements that are subjected to similar traffic and environmental conditions. To accomplish the overall goal, this study involved the following objectives:

- Evaluating the impact of stabilized base layers on the mechanical responses of flexible pavements (stresses and strains), as measured using the field Falling Weight Deflectometer (FWD) and layered elastic analysis results of five field sections in the state of Rhode Island.
- Conducting Pavement ME Design analyses of the five field sections to determine which of the four types of stabilized bases improved the overall performance of flexible pavements the most.

- Comparing the life cycle costs of each of the pavement sections containing the four different stabilized bases to that of the section containing the untreated base in order to determine which stabilized base was the most cost effective to use in flexible pavements.

Research Approach

The approach utilized to accomplish the overall goal of the study consisted of several tasks, which included:

Task 1: Conducting Falling Weight Deflectometer (FWD) tests on five field sections located on Rhode Island (RI) Route 165; one year after construction. These field sections contained a $CaCl_2$ stabilized base, Portland cement stabilized base, geogrid stabilized base, bituminous stabilized base, and a control, untreated RAP base. The purpose of this task was to obtain the pavement deflections of the five field sections after they were subjected to one year of trafficking.

Task 2: Backcalculating the elastic moduli of all the layers of the five field sections by analyzing the collected FWD data (or deflections) in the BAKFAA backcalculation software. The overall purpose of this task was to determine the stiffness (or elastic modulus) of each layer of the five field sections of RI Route 165 after one year of trafficking.

Task 3: Computing the critical pavement mechanical responses (i.e. the tensile strains at the bottom of the HMA layer and the compressive strains at the top of the subgrade layer) of the five field sections by conducting a layered elastic analysis using the Kenlayer software and the backcalculated layer moduli obtained for all the sections. This task also

involved computing the mechanical responses at the stage of crack initiation in a flexible pavement. The overall purpose of this task was to gain insight into fatigue cracking potential of the HMA layer and the total rutting expected in the structure of all the field sections.

Task 4: Comparing the impact of each of the stabilized/untreated bases on the overall predicted performance of the entire pavement section by conducting Pavement ME Design simulations. The purpose of this task was to determine which of the stabilized bases improved the fatigue and rutting performance of the entire pavement section the most.

Research Scope

Figure 1 below, shows an illustration of the five field sections evaluated in this study. These field sections were located on RI Route 165 between utility poles 304 and 521. These pavement sections are part of a controlled study currently being conducted by RI Department of Transportation (RIDOT) to evaluate their long-term field performance. Four of the five sections were constructed using stabilized base layers and one was constructed as a control section using an untreated RAP aggregates base. Four different stabilizing agents (i.e., calcium chloride, emulsified asphalt, Portland cement, and geogrids) were utilized to construct the four stabilized base layers. All these sections were constructed in 2013.

Falling Weight Deflectometer tests were conducted on all five pavement sections in July 2014; one year after construction. The BAKFAA software was used to backcalculate the elastic moduli of all the layers of each field section, from the pavement

deflections obtained during FWD testing. The Kenpave software was utilized to conduct a layered elastic analysis of each pavement section after one year after construction and at the point of crack initiation. The performance of the five pavement sections was predicted by performing AASHTOWare Pavement ME Design simulations.

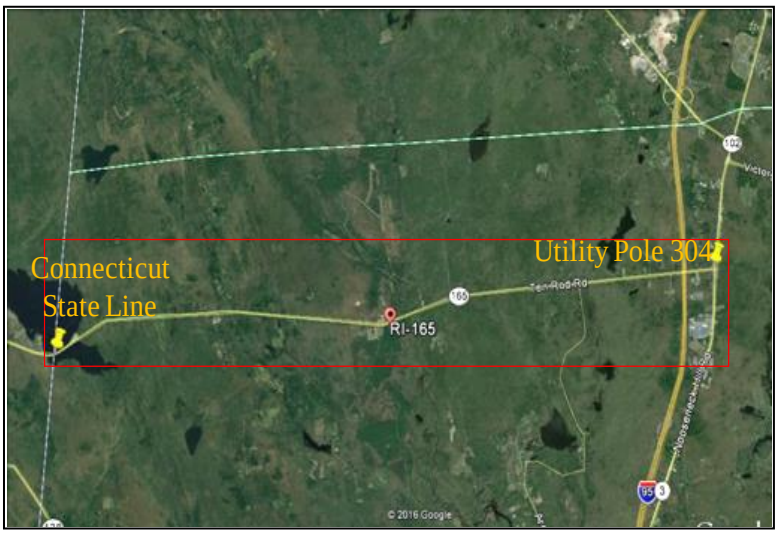

Figure 1. Field segment of RI Route 165 analyzed in this study

Chapter 2

Literature Review

This literature review is divided into three components. The first component of the literature review summarizes the findings of previous studies that have evaluated the laboratory performance and field performance of the stabilized bases evaluated in the study. The second component of the literature review provides a detailed description and background of FWD testing, backcalculation, the Kenlayer software, and the AASHTOWare Pavement ME software.

Performance of Stabilized Bases

Calcium chloride stabilized base. Calcium chloride is an alkaline earth metal salt that is most stable in the liquid state. It is a hygroscopic, deliquescent, chemical compound that absorbs and retains moisture for long periods. The capacity of calcium chloride to absorb moisture is heavily reliant on the temperature and relative humidity of the environment. Generally, the absorptive capacity of calcium chloride increases as the relative humidity of its environment increases [11]. Calcium chloride has traditionally been used in the pavements industry as a treatment to regulate dust formation in unpaved, low volume roads [12]. However, in recent time, the use of calcium chloride has been expanded to base/subbase layer stabilization in flexible pavements. As such, there have been numerous studies which have investigated the laboratory and field performance of calcium chloride stabilized bases/subbases to assess how these stabilized bases influence the overall performance of flexible pavements.

Kirchner et al. (1991) [13] conducted a study which evaluated the laboratory performance of reclaimed base courses stabilized with $CaCl_2$. In this study, the researchers compared the laboratory performance of the $CaCl_2$ stabilized base with the laboratory performance of an untreated aggregate base. The study involved a series of compaction tests which were carried out on both the untreated and $CaCl_2$ stabilized bases. The researchers also looked at the effect of various amounts of $CaCl_2$ on the reduction of frost heaving in soil mixes. Kirchner et al. (1991) [13] reported that the water absorbed by $CaCl_2$ in stabilized bases had a stronger moisture film when compared with the plain water in untreated bases. This stronger moisture film was mainly attributed to the alterations the $CaCl_2$ made to the moisture it absorbed. When the moisture was absorbed by the $CaCl_2$, the calcium chloride increased the surface tension and reduced the vapor pressure and freezing point of the moisture. It was reported that this strengthened moisture film, enhanced the lubrication between the base layer aggregates and enabled greater densities to be achieved with less compaction. Since compaction typically improves base layer stability and increases the bearing capacity and shear strength of base layer aggregate, calcium chloride stabilization was found to enhance the bearing capacity and shear strength of aggregate base layers [13].

In the study, Kirchner et al. (1991) [13] also reported that frost heave was eliminated when 0.5% of calcium chloride (by weight) was added to untreated aggregates of the $CaCl_2$ stabilized base. Since frost heave usually leads to permanent deformation in flexible pavements, $CaCl_2$ stabilization was found to reduce permanent deformation (i.e. frost damage) in aggregate base layers particularly during freeze-thaw cycles.

Shon et al. (2008) [14] conducted a study which evaluated the field performance aggregate base layers stabilized with Class C fly ash and $CaCl_2$. In this study the researchers investigated the effect of adding $CaCl_2$ to a fly ash treated roadbed during construction. Shon et al. (2008) [14] assessed the impact of the $CaCl_2$ on the setting time, compaction efficiency, and ultimate strength of the stabilized base. This study involved the construction of three full scale test sections which contained an untreated base, a stabilized base (treated with 1.3 $CaCl_2$ and 5% Class C fly ash), and a stabilized base (treated with 1.7 $CaCl_2$ and 5% Class C fly ash). The unconfined compressive strength and soil suction of the three aggregate bases were evaluated in the laboratory and dynamic cone penetrometer (DCP) tests were conducted on the full scale base sections after they were subjected to trafficking by a pickup truck.

Shon et al. (2008) [14]reported that the addition of the $CaCl_2$ to the fly ash stabilized bases resulted in increased and accelerated strength gains. The researchers also reported that the soil suction values of laboratory samples which contained $CaCl_2$ was higher than those that did not contain $CaCl_2$. Since higher suction values typically indicates a higher potential to increase compression between aggregate particles, the addition of $CaCl_2$ was found to increase the shear strength of the aggregates in the stabilized bases. Additionally, Shon et al. (2008) [14] found that the DCP index of the test sections decreased as $CaCl_2$ content increased. This indicated that the addition of the $CaCl_2$ to the fly ash treated bases also increased the stiffness of these layers.

In addition to the studies previously outlined, there have been numerous studies which have evaluated the laboratory and field performance of $CaCl_2$ stabilized bases. The key findings of some of these studies are outlined in Table 1 below.

Portland cement stabilized base. Portland cement (PC) is one of the most commonly utilized stabilizing agents [15]. Cement stabilization is independent of the aggregate and occurs during cement hydration; a process that involves a series of chemical reactions. Portland cement stabilized bases generally consist of a mixture of pulverized aggregate, Portland cement and water. Portland cement stabilized bases are usually compacted to a high unit weight and shielded against moisture loss for a specified curing period [16]. When the mixture of Portland cement, pulverized material, and water is cured, a hardened material is formed. The plasticity index and permeability of this hardened material is typically lower than that of untreated aggregates and the strength of the hardened material is generally higher than that of untreated aggregates as well [16].

Many studies have evaluated the effectiveness of using cement stabilized bases in flexible pavements. These studies have analyzed both the laboratory and field performance of cement stabilized bases. Jones et al. (2015) [17] conducted a study which compared the relative field performance of full scale test sections which underwent full-depth reclamation (FDR) with Portland cement and no stabilization. The test sections evaluated in the study were subjected to accelerated load testing using a heavy vehicle simulator (HVS) and the stiffness, cracking, rutting, and moisture susceptibility of the pavement sections were monitored. Jones et al. (2015) [17] reported that permanent deformation on the surface of the Portland cement FDR section was significantly lower than that of the non-stabilized FDR section after testing. This was because the terminal average maximum rut depth (13 mm) was met on the non-stabilized FDR section after 335,000 load repetitions while the average maximum rut recorded on the Portland cement FDR section was 3.0 mm after 1.5 million load repetitions. Jones et al. (2015) [17]

reported that no cracking was observed on either section after testing. The researchers also concluded that the stiffness of the recycled layer in the Portland cement FDR section was significantly higher than that of the non-stabilized FDR section before and after the sections were subjected to trafficking.

In addition to the study conducted by Jones et al. (2015) [17], numerous studies have been conducted to evaluate the field and laboratory performance of cement stabilized bases. The key findings of some of these studies are summarized in Table 1 below.

Table 1

Summary of key findings of previous studies which have evaluated the laboratory and field performance of cement stabilized bases

Author	**Key Findings**
Wang et al. (2010) [18]	• Shrinkage cracks which form during cement hydration negatively impact performance of cement treated bases. • Shrinkage stress in base layers increases as cement dosage increases. • Cement treated base containing a cement dosage of 3% to 4% had the lowest dry-shrinkage potential.
Singh et al. (2007) [19]	• Increase in cement content increases the maximum dry density (MDD) and decreases the optimum moisture content (OMC) of laboratory compacted cement stabilized fly ash bases. • MDD of cement stabilized fly ash bases is comparably lower than that of similarly graded natural soil. • Increase in cement content exponentially increases the CBR value of cement stabilized fly ash bases.
Taha et al. (2002) [20]	• Ability of RAP aggregates to function as a structural component of pavement is enhanced when they are stabilized with cement rather than blended with only virgin aggregate. • Cement stabilized RAP virgin aggregate mixtures appeared to be a viable alternative to dense graded aggregate in road base construction.

Geogrid stabilized base. A geogrid is a type of geosynthetic manufactured from synthetic polymer materials. Geosynthetics are generally used in flexible pavements to provide reinforcement, separation, filtration, and drainage. [21]. Geogrids are generally used in the subbase and granular layers of flexible pavements in order to provide reinforcement for those layers. Studies have found that geogrids limit the amount rutting and fatigue in flexible pavement [8]. This is generally attributed to three main mechanisms which are inherent in all geogrids. These mechanisms are: lateral confinement, increased bearing capacity, and the "tensioned membrane" effect.

Geogrids laterally confine base layer aggregates at the interface of the geogrid and base layer aggregate. The lateral confinement typically leads to the formation of frictional forces at the interface of the geogrid reinforcement and the aggregates in the base layer. When flexible pavements are subjected to vertical stresses due to traffic loads, base layer aggregates tend to shift laterally. This causes the base layer aggregates to transfer shear loads to the geogrid at the geogrid to aggregate interface, which in turn creates tensile forces in the geogrid [8]. The horizontal tensile strains in the base layer are then reduced by the tensile strength of the geogrid as illustrated in Figure 2 below. Additionally, the horizontal confinement created by geogrid reinforcement also increases the average stress of the base layer aggregates and this in turn increases the shear strength of these aggregates.

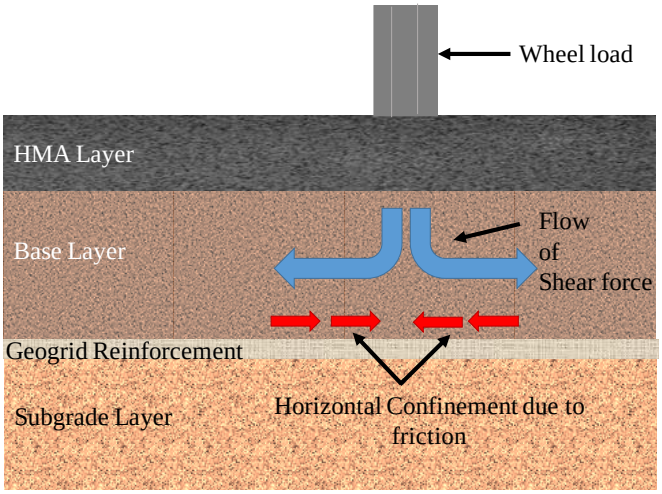

Figure 2. Lateral confinement mechanism of geogrid: (Zornberg et al. (2010) [8])

The increased bearing capacity mechanism in geogrids enables them to provide additional reinforcement for the base layer aggregates of flexible pavements. The reinforcement provided by geogrids creates an alternative surface (plane) of failure in the base layer where there is increased bearing capacity [8]. This is shown in Figure 3 below. This alternative plane of increased bearing capacity reduces the magnitude of the shear stresses transferred to the subbase or subgrade layers and provides additional vertical confinement outside the area loading in the base layer.

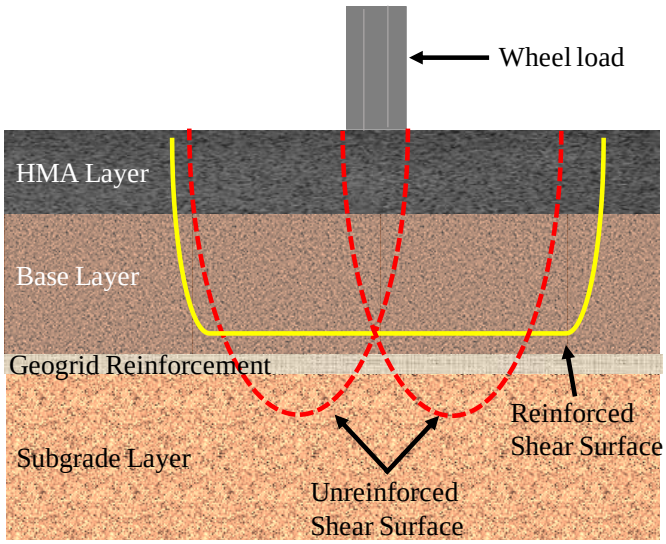

Figure 3. Increased bearing capacity mechanism of geogrid: (Zornberg et al (2010) [8])

In addition to providing confinement, geogrids provide support for wheel loads through the "tensioned membrane" effect. Geogrids act similar to tensioned membranes when there is significant deformation in flexible pavements. Geogrids develop a concave shape when there is large permanent deformation as shown in Figure 4 below. When traffic loads are applied directly in the wheel paths of flexible pavements, geogrids provide vertical reactive forces which support the wheel loads. These vertical reactive forces also cause the compressive stress on the subgrade layer to decrease [8]. Large deformations in the pavement are usually required in order to mobilize the tension in the geogrid which creates these reactive forces.

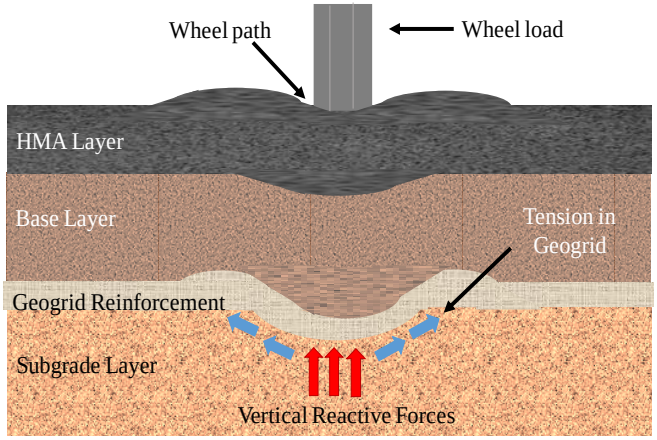

Figure 4. Tensioned membrane mechanism of geogrid: (Zornberg et al. (2010) [8])

A study by Abu-Farsakh et al. (2011) [22] evaluated the laboratory performance of geogrid reinforced bases in flexible pavements using cyclic plate load testing. Four different types of geogrids with different geometries, mechanical properties, and physical properties were utilized in the study. A cyclic load was applied to flexible pavement test sections which were constructed with and without geogrid reinforcement inside a box. Testing was conducted on two unreinforced sections, four reinforced sections; with a geogrid layer placed at the base/subbase layer interface, two reinforced sections; with one geogrid layer placed at the middle third of the base layer, and a reinforced section; with one geogrid layer placed at the upper one third of the base layer. These cyclic plate load tests were carried out in order to evaluate the impact of the geogrid geometry, location and tensile strength on the stress distribution and permanent vertical strain in the subgrade. Testing results, according to Abu-Farsakh et al. (2011) [22], indicated that use of geogrid base reinforcement extended the service life of flexible pavement sections. The researchers also determined that the use of geogrids in the upper one third of the base layer improved the overall performance of the stabilized base. Additionally, Abu-Farsakh

et al. (2011) [22] concluded that geogrid helped to redistribute the applied loads over a wider area on top the subgrade. This caused less permanent deformation to accumulate in the subgrade and reduced the overall rut depths of the pavement.

Wu et al. (2015) [23] conducted a study which evaluated the effect of geogrid reinforcement on unbound granular pavement base materials. Four types of geogrids; with different apertures and strengths were evaluated in the study. Two of the geogrids evaluated in the study consisted of two and three layers of high strength, biaxial, polypropylene respectively while the other two geogrids consisted of a single layer of punched-drawn biaxial polypropylene. Loaded wheel tester (LWT) tests were conducted on compacted base course specimen to simulate actual service conditions and the rut depths of the base specimen and were measured along the loading path. Cyclic plate load tests were also conducted on the geogrid reinforced base course specimen. Testing results according to Wu et al. (2015) [23] indicated that the rut depths of all the geogrid reinforced base layer specimen was less than that of the control specimen with no reinforcement. The researchers reported that the triple layered high strength, polypropylene geogrids showed significant improvement in reinforcement when it was used in river sand bases while the single layered, biaxial polypropylene geogrid was the most effective geogrid in reinforcing grave bases.

Bituminous stabilized base. The modification of untreated soil material (aggregates) by emulsified asphalt is referred to as bituminous stabilization. Bituminous stabilization of base layer aggregates generally consists of a three stage process. This process includes the blending of aggregates, compaction, and the application of emulsified asphalt. The base layer aggregates are initially blended in order to alter the

gradation of the in place material. This change in aggregate gradation facilitates compaction; which is performed to increase aggregate interlock in the base layer [4]. Emulsified asphalt is added to the untreated base layer aggregates in order to increase soil strength through aggregate adhesion. Bituminous stabilization generally decreases the soil permeability of base layers in flexible pavements and increases aggregate interlock, soil strength, and durability.

Cold recycling is a common method used to stabilize base layers with emulsified asphalt. The process of cold recycling involves milling, mix design, binder addition, placement, compaction, and quality assurance [24]. The emulsified asphalt in cold recycled asphalt functions as an adhesive agent while the aggregates usually consist of the RAP. Studies have shown that the performance of cold recycled asphalt base layers can be improved by using additives such as fly ash, cement, and lime [4]. However, other studies have indicated that the presence of aged binder around the RAP aggregates can cause cold recycled asphalt bases to perform poorly.

Wu et al. (2006) [25] conducted a study to evaluate the field performance of foamed asphalt base materials. This study involved accelerated pavement testing on three identical, full-scale test sections. The base layer of the control test section in the study consisted of crushed stone and the base layer of the other two test sections consisted of a foamed asphalt blend. A 50% RAP and 50% recycled soil cement foamed asphalt blend was used in the base layer of one test section and a 100% RAP foamed asphalt blend was used in the base layer of the other test section. The accelerated pavement testing was performed using an accelerated load facility (ALF) wheel assembly and the surface

deflections, surface rut depths and cracking maps of the full scale test sections were monitored during testing.

The results of the testing according to Wu et al. (2006) [25] indicated that the foamed asphalt bases performed similarly under the initial load level of 43.4 kN and this performance was found to be better than that of the crushed stone base. However, the researchers reported that the rutting rates on both foamed asphalt bases was higher than that of the crushed stone base when the load level was increased. Wu et al. (2006) [25] determined that the high rutting rates on the (50% RAP and 50% recycled soil cement) foamed asphalt base test section was due to the water susceptibility and weak aggregate skeleton of the foamed asphalt base. The researchers also determined that the high rutting rates on the (100 % RAP) foamed asphalt base test section was due to the poor water resistance and over asphalting of the foamed asphalt base.

Lane et al. (2012) [26] conducted a study which evaluated the long term performance of a flexible pavement which underwent a full depth reclamation with expanded asphalt. The study involved the construction of a full depth reclamation with expanded asphalt stabilization on the Tans Canada Highway between the cities of Sault Sainte Marie and Wawa, in Northern Ontario, Canada. The study evaluated three highway sections which were constructed with different expanded asphalt mix designs and a control section which was constructed with HMA. The researchers monitored the field sections annually for 10 years using an Automated Road Analyzer (ARAN) which measured rutting and IRI.

Lane et al. (2012) [26] reported that the pavement remained smooth on the expanded asphalt sections since in the IRI was less than 1 after 10 years. The researchers also reported that the condition of the expanded asphalt sections was excellent since the Pavement condition index (PCI) was greater than 85 after the 10 year evaluation period. Lane et al. (2012) [26] concluded that the control section deteriorated at a much faster rate than the expanded asphalt stabilized pavement sections during the 10 year period.

Background of Testing and Analysis Procedures

Falling Weight Deflectometer testing. Falling Weight Deflectometer testing is a nondestructive method of testing used to obtain the deflection basin of flexible pavements. A Falling Weight Deflectometer is a deflection testing instrument which operates based on the impulse loading principle [27]. In FWD testing, a drop weight or variable load is released from set heights and allowed to fall under gravity onto cylindrical shock absorbers. These shock absorbers then transfer an impulse load to a spring loaded plate which rests on the surface of the pavement. The variable load is typically 9000 lb (40kN) and the diameter of the spring loaded plates is usually 11.82 in. (30cm) [27]. The pavement response to the impulse load (i.e. deflections is measured using seven velocity transducers (geophones) that are placed at specific radial distances from the center of the applied load or plate [27]. These radial distances are usually given the designations D_0, D_1, D_2, D_3, D_4, D_5, and D_6 [28]. The maximum pavement deflection is recorded directly under the load at the D_0 location and the remaining six geophones are generally placed radially out from the center of the load at 12 in (30.48 cm) intervals [28]. Therefore the D_1 geophone is placed at 12 in from the center of the load and the D_6

geophone is placed 72 in (182.88 cm) from the center of the load. A typical setup of FWD testing is shown in Figure 5 below.

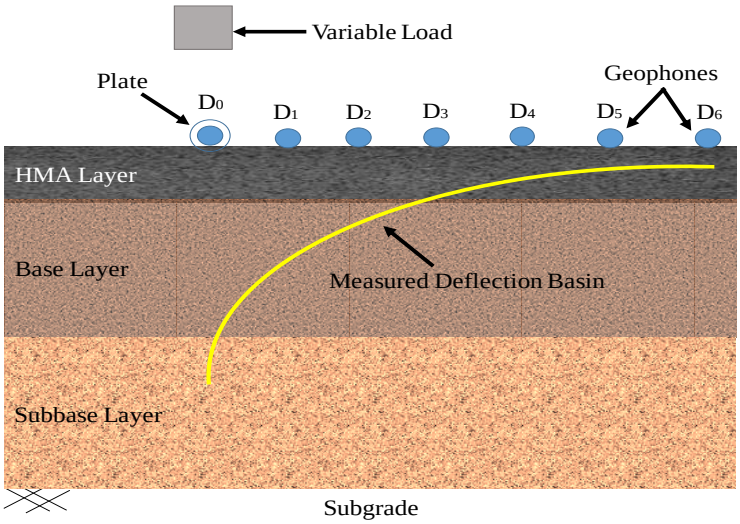

Figure 5. Schematic of Falling Weight Deflectometer testing: (Mehta et al. (2003) [27])

Backcalculation. Backcalculation is often referred to as the "inverse" problem of determining material the properties (i.e. layer moduli) of a flexible pavement from its response to surface loading [27]. Backcalculation is an ill-posed process in which iterative or optimization methods are utilized to compute theoretical deflections. These deflections are calculated by varying the layer moduli of the pavement until a tolerable "match is made with measured field deflections obtained from FWD testing [29]. Backcalculation is based on the half-space theory where a pavement is assumed to be a homogenous, isotropic, linear-elastic half-space [30].

Computer programs are usually used to perform backcalculation of multi-layered systems. These computer programs allow users to input estimated initial or "seed" moduli

values for the various layers of a pavement. A subroutine program within the backcalculation software utilizes a particular type of analysis (finite element or multi-layer) to compute the corresponding theoretical deflections based on the inputted moduli values [29]. The final layer moduli outputted by the backcalculation software represents an "effective" layer moduli which adjusts for stress-sensitivity and discontinuities. The allowable range of the computed layer elastic moduli depends on the computer software used to perform the backcalculation [29].

The BAKFAA backcalculation software. BAKFAA is a backcalculation computer software developed by the Federal Aviation Administration (FAA). This software is used by the FAA to analyze field deflections of airport pavements. The subroutine program in the BAKFAA software computes theoretical deflections by matching the radius of curvature of the measured and calculated deflection basins. This minimizes the error between the calculated and measured deflections. Matching the radius of curvature of the computed and measured deflection basins ensures that more representative elastic moduli values are outputted by the software because the pavement stiffness is strongly related to the radius of curvature of the deflection basin [29]. The analysis of deflection data with the BAKFAA software stops when the error value between the radius of curvature of the measured and calculated deflections is less than or equal to a minimum threshold value. The allowable range for the computed deflections or elastic moduli in the BAKFAA software is (+/-) 20%.

The Kenlayer software. Kenlayer is a component of the Kenpave computer program; which consists of a suite of pavement analysis and design software. The Kenlayer software is a computer program commonly used to compute the stresses and

strains in elastic multilayered systems that are subjected to circular loads. Generally, the solutions provided by Kenlayer analyses can be superimposed for multiple wheel loads, applied iteratively for non-linear layers, and collocated at various periods for viscoelastic layers [31]. Hence, this software can be used to analyze single and multiple wheel loads acting on pavements with elastic, viscoelastic, linear or nonlinear layers.

The analyses performed by Kenlayer software are based on the layered elastic theory. The layered elastic theory assumes that the stress, strains, and deflections created by concentrated loads can be integrated to obtain the mechanical responses created by a circular loaded area [31]. Several other assumptions are made in linear elastic analyses. These assumptions include: a) the stress in each pavement layer is proportional to the strain in accordance with Hooke's Law; b) each pavement layer (with the exception of the lowest layer) is finite, homogenous, and isotropic; c) the pavement extends infinitely in the vertical and horizontal directions; d) the vertical and horizontal displacements of pavement material is continuous across the layer interfaces [31].

AASHTOware Pavement ME software. The AASHTOware Pavement ME software is based on the mechanistic-empirical design approach to flexible pavements. This approach to flexible pavement design involves the use of mechanistic models to predict pavement performance. The AASHTOware Pavement ME software was developed to incorporate the effect of climate, material properties, traffic, and damage accumulation when designing flexible pavements. The software uses an iterative process to predict the level of distress that may arise in a flexible pavement. This iterative process uses stresses, strains, and deflections to determine the incremental damage that may accumulate in a pavement structure over its design life [32]. The level of pavement

distress predicted by the AASHTOware Pavement ME software is set against reliability values which determine whether the flexible pavement passes specific distress criteria.

The AASHTOware Pavement ME software allows users to input three levels of hierarchal inputs based on the method the users utilized to obtain the resilient moduli of the pavement layers. Level 1 inputs are entered in the software if the resilient moduli of the pavement layers were obtained from site specific testing, level 2 inputs are used in Pavement ME if the resilient moduli were obtained from correlations with standard tests and level 3 moduli are utilized in the software if the resilient moduli obtained were obtained from local or national default values [32]. The software also permits users to specify the amount of vehicles that are expected to traverse the pavement based on their vehicular classification. It then uses the traffic data inputted by the user to replicate the traffic conditions that a flexible pavement may typically experience throughout its design life. An illustration of the vehicle classifications used in the AASHTOware Pavement ME for analysis is shown below in Figure 6.

The AASHTOware Pavement ME software also utilizes an Enhanced Integrated Climatic Model (EICM) to simulate the moisture, temperature, and freezing conditions that a flexible pavement may be subjected to throughout its design life [32]. The EICM includes weather databases from the National Oceanic Atmospheric Administration (NOAA) and the soil index from the long term pavement performance (LTPP) program and the United States Geological Surveys (USGS). The EICM accounts for the monthly air temperature and precipitation a pavement will experience by using data from the weather station closest to the pavement. The software allows the user to specify the

weather station that is nearest to the pavement prior to the AASHTOware Pavement ME analysis.

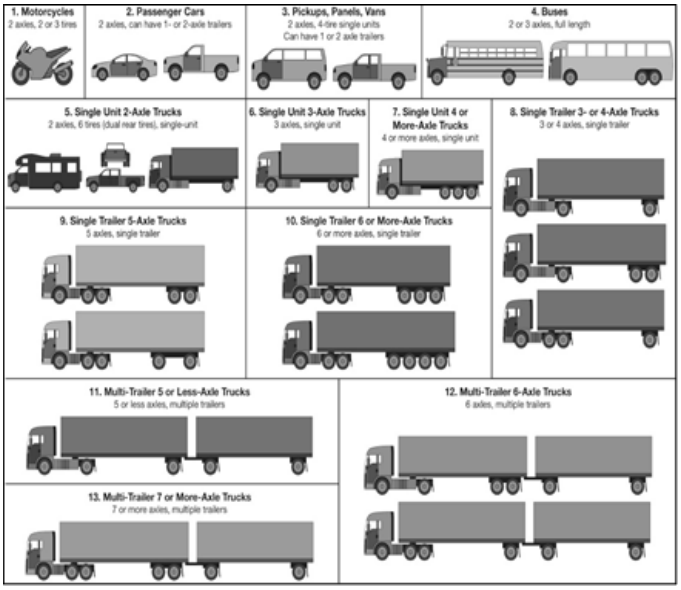

Figure 6. Vehicle classifications based on number of axles

Chapter 3

Pavement Sections, Analysis Procedures & Inputs

This section outlines the construction and analysis procedures utilized to evaluate the pavement sections considered in the study. Five field sections located on Route 165 (between utility poles 304 and 521) in Rhode Island (RI) were evaluated in this study. These sections are part of a controlled study currently being conducted by RI Department of Transportation (RIDOT) to evaluate their long-term field performance. Four of the five sections were constructed using stabilized base layers and one was constructed as a control section using untreated Reclaimed Asphalt Pavement (RAP) aggregates base. Four different stabilizing agents (i.e., calcium chloride, emulsified asphalt, Portland cement, and geogrids) were utilized to construct the four stabilized base layers. All these sections were constructed in 2013. Figure 7 presents the typical pavement structure utilized in all five sections selected for this study.

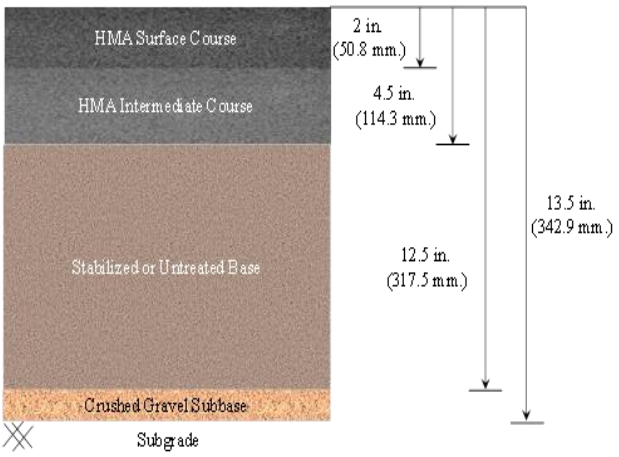

Figure 7. Pavement structures of all five pavement sections

Geology of Rhode Island Route 165

RI Route 165 was initially constructed on soft, swampy soil. During its reconstruction in 1986, soil material that was unconducive to pavement construction was removed, and an embankment was floated on the soft soil. The natural soil at the time of reconstruction contained deposits of sand, gravel, silt, peat, and organic silt [33]. Based on the results of boring tests, researchers concluded that RI Route 165 was constructed on glacial till and stratified kame [33]. The natural soil beneath RI Route 165 has a plasticity index of zero, a low shrink-swell capacity, and a soil classification that ranges from A-1 to A-4 (based on the AASHTO soil classification). It is important to note that the natural soil has a high water table due to the presence of granite near its surface as well as a high susceptibility to frost action.

Rhode Island Route 165 Pavement Section Overview

As can be seen from in Figure 7 above, all sections of RI Route 165 have a 4.5 in. (114.3 mm) HMA pavement layer (i.e., 2 in. (50.8 mm) surface and 2.5 in. (63.5 mm) intermediate courses). The base layers (treated or untreated) in all sections had a thickness of 8 in. (203.2 mm) (Figure 7) and was overlaid on top of a 1 in. (25.4 mm) crushed gravel subbase layer. In addition to having the same pavement structure (i.e., similar layer thicknesses), the gradation of the base layers of all the test sections was similar; with 95% to 100% passing the No.3 sieve (0.265 in. (6.7 mm)) and 2% to 15% passing the No.200 sieve (0.0029 in. (75 μm). Additionally, all sections were subjected to the same traffic and environmental conditions. This is the case because all sections are located adjacent to each other along RI Route 165. Since traffic and environmental

conditions as well as pavement structure for all sections were similar the impact of base type on overall performance of these sections can be investigated. This is because the only difference in the pavement sections was base layer type. The following subsections provide a discussion of the materials and procedures used to construct the base layers in each of these sections.

Section containing calcium chloride ($CaCl_2$) stabilized base. The section containing the $CaCl_2$ treated base is 9332 ft. (≈ 2844 m.) long starting at utility pole 304 and ending on utility pole 369 on RI Route 165. This section underwent a Full Depth Reclamation (FDR) process in which a $CaCl_2$ solution, prepared in accordance to AASHTO M144 standards "Standard Specification for Calcium Chloride," was utilized to stabilize the base layer (8 in. thick in Figure 6 above). This solution consisted of approximately 35 % ± 1% alkali chloride, 2% sodium chloride, and 0.1 % magnesium chloride. A total volume of 0.8 gallons per square foot (3.40 L/m^2) of $CaCl_2$ solution was applied to and mixed with the reclaimed aggregates to a depth of 7.87 in (20 cm) using a pressure distributer. The rate of application was 0.1 to 2 gallons per square yard [33]. Vibratory sheep foot rollers and motorized graders were utilized to grade and compact the $CaCl_2$ treated aggregate. The compaction quality was deemed satisfactory when the field density was approximately 95% or higher than that measured in the laboratory (i.e., Proctor density). The dry density of the $CaCl_2$ stabilized base was 131.1 lb/ft^3 (20.6 kN/m^3). It is important to note that the target in place density was the same for all the field sections. It is also noteworthy that the same grading and compaction equipment were utilized to compact all base layers for all five sections considered in this study.

Control section containing untreated (RAP) base. The control section containing the untreated RAP base layer is a 2650 ft. (≈ 808 m.) long starting a utility pole 369 and ending at utility pole 400 on RI Route 165. Similar to the section containing the $CaCl_2$ base discussed above, the control section also underwent a FDR process in which the existing pavement was pulverized and used as aggregates for constructing an untreated base [33]. These untreated reclaimed aggregates were then compacted using the equipment discussed above. The dry density of the untreated RAP base was 129.1 lb/ft^3 (20.4 kN/m^3).

Section containing Portland cement stabilized base. The section containing the Portland cement stabilized base is approximately 15700 ft. (≈ 4785 m.) long starting at utility pole 400 and ending at utility pole 506 on RI Route 165. This section underwent a FDR process in which Portland cement was utilized to stabilize the base layer. The FDR process involved the pulverization and blending of existing RAP aggregates using a reclaimer followed by the addition of 3.5 lb./ft.^{2} (17.4 kg/m^2) or 4% by total sample weight of Portland cement [34]. A cement spreader was used to distribute dry cement over the over the pulverized material. The cement spreader contained a tractor trailer with a pressure controlled "Drop behind system". This system was calibrated daily to ensure that 3 lbs/yd^2 (1627.5 g/m^2) of dry cement was distributed over the pulverized material [33]. Water was then supplied to the mixing chamber of the reclaimer via a water truck, and the reclaimer was passed over the pulverized material (a second time) in order to mix the cement-treated material to a required depth [34]. After the cement treated material was mixed, it was compacted and graded. The dry density of the cement stabilized base was 127.3 lb/ft^3 (20.0 kN/m^3).

Section containing geogrid stabilized base. The section containing the geogrid stabilized base geogrid base segment is approximately 3500 ft. (≈ 1066 m.) long starting at utility pole 506 and ending at utility pole 518 on RI Route 165. This section underwent mechanical stabilization using geogrids. The type of geogrid utilized was manufactured from polypropylene and had triangular apertures. The selected geogrid was used as reinforcement in bases constructed using the pulverized aggregates [33]. The goal of using geogrids was to evaluate the potential benefits of using geogrids in stabilizing aggregate base layers. The dry density of the geogrid stabilized base was 129.9 lb/ft^3 (20.4 kN/m^3).

Section containing bituminous stabilized base. The section containing the bituminous stabilized asphalt base is 6600 ft. (≈ 2012 m.) long starting at utility pole 518 and ending at the Connecticut state line. This section underwent a FDR process in which asphalt emulsion, prepared in accordance to AASHTO T-40 standards "Standard Specification for Asphalt Emulsion Sampling, Storage, and Handling," was utilized to stabilize the base layer. The type of asphalt emulsion used to stabilize the base layer was an anionic medium to rapid setting (HFMS-2) asphalt emulsion [33]. The asphalt emulsion was heated to between 212F to 248 F (100^{o}C and 120^{o}C), mixed thoroughly into the base layer during the FDR, and allowed to cure for 5 days. The asphalt emulsion was applied using a spray nozzle and then mixed uniformly with the pulverized aggregate materials reclaimed from existing pavement. The mixture was then compacted using the previously discussed equipment. The dry density of the bituminous stabilized base was 126.1 lb/ft^3 (19.8 kN/m^3).

Falling Weight Deflectometer Testing Procedure

Falling Weight Deflectometer (FWD) tests were conducted on the westbound and eastbound directions of all the sections discussed above. These tests were conducted in July 2014. The pavement temperature at the time of testing was 70°F (21.1°C). The FWD tests were carried out by applying four loads (i.e., 6612 lbs [≈29.4kN], 9256 lbs [≈41 kN], 13,224 lbs [≈58.8 kN], and 17,631 lbs [≈78.4 kN]) to the pavement sections and measuring deflections at varying locations from the center of the applied loads. The loads were allowed to fall under gravity onto two plates which contained (9+9) buffers. The radius of these plates was 5.91 in. (150 mm). The 6612 lbs (≈29.4 kN) load was initially applied to the pavement sections followed by the 9256 lbs (≈41 kN), 13,224 lbs (≈58.8 kN), and 17,631 lbs (≈78.4 kN) loads. The pavement deflections were then measured using seven geophones. These geophones were placed that were placed at 0 in. (0 mm), 7.87 in. (≈200 mm), 11.81 in. (≈300 mm), 17.72 in. (≈450 mm), 23.62 in. (600 mm), 35.43 in. (≈900 mm), and 47.24 in. (1200 mm) away from the center of the load.

There were forty six points of FWD testing in total conducted along the five sections of RI Route 165 immediately after construction. There were 10 test points on the $CaCl_2$ stabilized base section of the highway; five in the westbound direction and five in the eastbound direction. There were six locations on the untreated (control) base section with three test points in both the westbound and eastbound directions. On the cement stabilized base section, there were eight test points in both directions of travel (i.e. the westbound and eastbound directions). There were six points of FWD testing on the geogrid stabilized base section; three in the eastbound direction and three in the

westbound direction. There were also eight points of FWD testing on the bituminous stabilized section with four test points in both the westbound and eastbound directions.

Backcalculation Procedure and Inputs

The BAKFAA software was used to analyze the pavement deflections obtained from the FWD testing at the various test locations along RI Route 165. These deflections are shown in Appendix A. The backcalculated layer moduli of all the pavement sections were obtained from the analysis of the July 2014 FWD data. The following procedure explained below was utilized to backcalculate the layer moduli of all the pavement sections:

a. Fix the subgrade modulus value so that the computed and measured deflections at the sensor 7 in Figure 8 (i.e. the geophone furthest from the applied load) matched. If the backcalculated subgrade moduli values along a pavement section were within 15% of each other, the average of these values were locked as the subgrade modulus for that entire pavement section. This guaranteed that the subgrade modulus values along individual pavement sections were consistent.

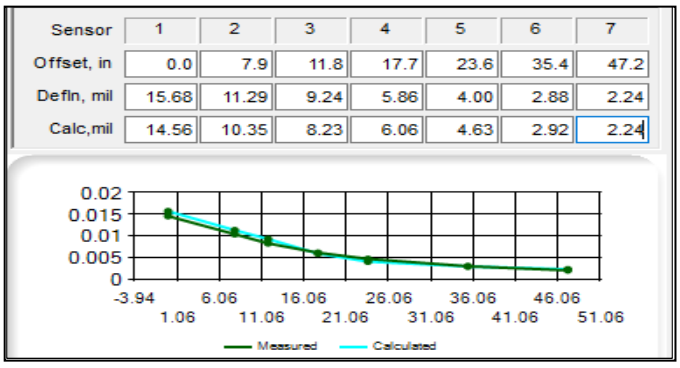

Figure 8. Measured and calculated deflections in BAKFAA software

b. Fix the subbase, base and HMA moduli values so that the computed and measured deflections at sensor 5, sensor 4, or sensor 3 exactly matched. If the backcalculated subbase, base, and HMA layer moduli along a pavement section were within 20%, the average backcalculated modulus value for each pavement layer was determined. These average values were then locked as the subbase, base, and HMA layer moduli of the pavement section. It is important to note that more variability was allowed in the backcalculated moduli of the upper layers (i.e. HMA, base and subbase layers) because they take the majority of the load [35]. Therefore it was expected that there would have been naturally more variability in these layers.

c. Ensure that there was no swapping or crossover between the measured and calculated deflection basins. This step guaranteed that the radius of curvature of both the measured and calculated deflections was similar. Swapping refers to a situation where the computed deflections in a pavement layer are noticeably higher than the measured deflections while the computed deflections in the pavement layer above is markedly lower than the measured deflections. Swapping causes the backcalculated modulus in a pavement layer to be higher than backcalculated modulus in the neighboring layer above. When swapping occurred, an iteration was performed with the two layers combined and an equivalent backcalculated modulus was obtained for both layers [27].

Kenpave Analysis Procedure and Inputs

A layered elastic analysis of the pavement sections was performed using the Kenpave software; a layered elastic analysis software .The backcalculated layer moduli

for each pavement section were used as inputs for the layered elastic analysis. The layered elastic analysis was performed to compute critical pavement mechanical responses in the pavement sections. These mechanical responses included the tensile strains at the bottom of the HMA layer, the compressive strains at the top of the subgrade layer and the total vertical displacement for the entire pavement structure. The bottom of the HMA layer is located 4.5 in. (114.3 mm) from top surface of the pavement sections and the top of the subgrade is located 13.5 in. (342.9 mm) from top surface as well. This is illustrated in Figure 7. The tensile strains at the bottom of the HMA layer were computed because they usually provide insight into fatigue cracking potential within that layer [1]. The compressive strains and total vertical displacement were also computed because they both provide indications about the total rutting expected in the pavement structure [1].

In addition to the computing the mechanical responses from backcalculated moduli immediately after construction (i.e. FWD data obtained in July 2014), the mechanical responses were also computed at the stage of cracking initiation in a flexible pavement. Researchers [36] have reported that this stage (i.e., crack initiation in flexible pavements) occurs when the moduli values of the HMA layers are reduced by 50% from their initial values immediately after construction. It is important to note that the 2014 backcalculated moduli values were considered as the "initial" (or immediately after construction) values in this study, despite the fact that the sections discussed above were constructed in 2013. The 2014 backcalculated moduli values were considered as the initial moduli values because no FWD testing was conducted at the time of constructing

the sections. Kenlayer was also utilized to compute the critical mechanical responses at the stages of crack initiation.

An 18-kip (≈ 80 kN) load was utilized in the Kenlayer analysis to compute the selected mechanical responses. Comparisons between the Kenlayer outputs (i.e., critical mechanical responses) were then carried out to determine the impact of the varying base stabilizing agents (or stabilized base) on pavement performance.

Pavement ME Design Simulation Inputs

Pavement ME Design simulations were conducted in order to compare the impact of each of the bases (stabilized or untreated) on the overall predicted performance of the entire pavement section. The inputs utilized in these simulations were level 3 inputs. To determine a vehicle class distribution that was representative of traffic on RI Route 165, data collected from Weigh in Motion (WIM) stations in close proximity to Route 165 were analyzed. The moduli values backcalculated from the 2014 FWD data were also utilized as inputs in the Pavement ME Simulations along with the layer thicknesses presented in Figure 7 above. In addition, climate data obtained from a weather station located in Providence, RI were used as inputs for the Pavement ME Design simulations. Table 2 below presents a summary of all inputs utilized in conducting the Pavement ME Design simulations. Upon completion of the Pavement ME Design simulations, the predicted rutting and fatigue cracking performance measures were compared for all sections to evaluate the impact of the various stabilizing agents (or stabilized base layers) on overall pavement performance.

Table 2

Summary of Pavement ME design inputs

Vehicle Class	Distribution (%)	Other Inputs	
Class 4	06.62	AADT	5800
Class 5	68.59	AADTT	240
Class 6	09.37	Traffic Growth Rate (%)	1.3
Class 7	01.64	HMA Thickness (in.)	4.5
Class 8	03.41	Base Thickness (in.)	8
Class 9	10.10	Subbase Thickness (in.)	1
Class 10	00.23	Surface Course HMA Binder Grade	PG 64-28
Class 11	00.00	Intermediate Course HMA Binder Grade	PG 64-22
Class 12	00.00	Base Modulus (psi)	Varies*
Class 13	00.04	Subbase Modulus (psi)	Varies*

Chapter 4

Results, Analysis & Discussion

Backcalculated Moduli Values

The results of the backcalculation analysis procedure implemented in this study to determine the values of the layer moduli for the five pavement segments are presented in this section. The average backcalculated moduli for the HMA, base, subbase, and subgrade layers of all the pavement sections (i.e. the $CaCl_2$ stabilized, the untreated, the cement stabilized, the geogrid stabilized, and the bituminous stabilized base sections) are presented in Table 3 below. The coefficient of variation between the backcalculated layer moduli for each layer along the five pavement section is also presented in Table 3.

Based on the results illustrated in Table 3, it can be concluded that the coefficient of variation between the backcalculated subgrade moduli along each pavement section is less than/or equal to 0.15 (or 15%). These results indicate that the values of the backcalculated subgrade moduli along individual pavement sections are consistent. It is also important to note that the average percent difference between the backcalculated subgrade moduli of all the pavement sections analyzed is 19.4%. This implies that the moduli values for the subgrade layer are relatively consistent across all five pavement sections since the allowable range for computed deflections in the BAKFAA software is +/-20%. Additionally, the backcalculated moduli values of the HMA, base, and subbase layers along each pavement section are also consistent since the coefficient of variation between the moduli values for these layers is less than or equal to 0.20 (20%) on each section. This coefficient of variation falls within the +/-20% allowable range for

computed deflections in the BAKFAA software. As was mentioned previously, a larger variability was expected in the HMA, base and subbase layers of the pavement sections because these layers were subjected to the majority of the applied load.

Table 3

Average backcalculated layer moduli values for each pavement section immediately after construction

Pavement Section	**Backcalculated Layer Moduli, psi**			
	HMA	**Base**	**Subbase**	**Subgrade**
(Control) Untreated RAP Base	255,771	35,663	31,924	35,122
Coefficient of Variation	0.09	0.15	0.06	0.11
Bituminous Stabilized Base	199,219	43,711	36,502	28,230
Coefficient of Variance (%)	0.17	0.06	0.16	0.15
$CaCl_2$ Stabilized Base	430,625	37,948	43,471	39,364
Coefficient of Variation	0.06	0.13	0.01	0.14
Cement Stabilized Base	316,440	126,817	43,536	31,736
Coefficient of Variation	0.20	0.06	0.10	0.11
Geogrid Stabilized Base	286,250	24,102	33,287	28,627
Coefficient of Variance (%)	0.00	0.10	0.01	0.15

Validation of backcalculated base layer moduli. The backcalculated base layer moduli for all sections were verified by comparing the average base layer modulus value along individual pavement sections to results obtained from a previous study [37]. In that study, the resilient moduli of samples of the same stabilized/untreated base layers considered in this study were investigated. The researchers prepared 5.90 in. (15 cm)

diameter specimens of the stabilized/untreated bases by blending virgin and RAP aggregates from the full depth reclamation on RI Route 165 and applying treatment to the RAP blends in accordance with RIDOT project specifications. The researchers then compacted the specimen and conducted cyclic triaxial tests on the samples. The triaxial tests consisted of two phases in which a uniform cyclic stress was applied for 500 compression cycles and a varying cyclical stress was applied for 15 compression cycles [37]. The confining pressures ranged from 2.9 psi to 20.0 psi (20 kPa to 138 kPa) while the cyclic stress amplitudes ranged from 2.9 psi to 40 psi (20 kPa to 275 kPa). From the laboratory tests, the range of the resilient modulus for each base (stabilized/untreated) was obtained. The backcalculated and laboratory-measured moduli values for all base layers considered in the study are shown in Table 4 below.

As illustrated in Table 4, the backcalculated base layer modulus of each pavement section falls within the range of laboratory-measured moduli values obtained from samples of corresponding pavement sections. This suggests that the backcalculated moduli values for the base layers are appropriate for use in additional analyses. This also implies that the backcalculated moduli values of the layers below the base layer (i.e. the subbase and subgrade) are also suitable for the analysis because the base layer modulus is strongly influenced by the modulus of these layers [27]. Since the backcalculated moduli values of the base, subbase, and subgrade layers are appropriate for the analysis, these layers values are therefore validated.

Table 4

Backcalculated and laboratory-measured moduli values for base layers

Base Layer	Backcalculated Moduli, psi	Laboratory-Measured Moduli, psi*
(Control) Untreated RAP Base	35,663	24,802 to 83,832
Bituminous Stabilized Base	43,711	25,672 to 53,809
$CaCl_2$ Stabilized Base	37,948	34,229 to 82,381
Cement Stabilized Base	126,817	76,580 to 275,282
Geogrid Stabilized Base	24,102	24,802 to 83,832

Comparison of backcalculated layer moduli of pavement sections. A comparison of the backcalculated moduli values of all the pavement sections immediately after construction is presented in Figure 9 below. The results presented in this figure indicate that the HMA layers in all the pavement sections had the highest moduli values. This trend, (i.e. the HMA layers having the highest moduli values) was expected because the HMA layers of flexible pavements are usually constructed with better-controlled and better-performing materials when compared to other layers. Figure 9 also illustrates another trend in which the base layer of all the pavements sections had the next highest backcalculated stiffness. This trend is also due to the fact that higher quality aggregates are used in the upper layers of flexible pavements.

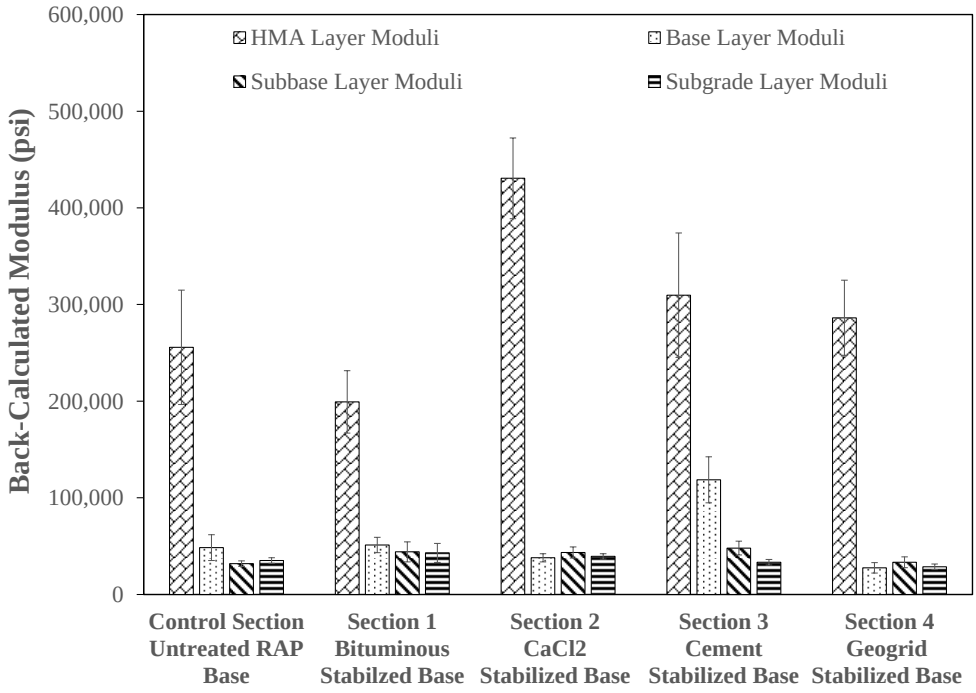

Figure 9. Comparison of backcalculated base layer moduli of all pavement sections one year after construction

Better performing aggregates are usually used closer to the surface of flexible pavements in order to ensure and maintain efficient load transfer between aggregates, while aggregates of an inferior quality compared to those in the upper layers, are used in the lower layers in order to reduce construction costs. If poorly performing aggregates are used in the upper layers of flexible pavements, there will be an increased risk of aggregates failing under traffic loads. When this occurs, the stresses due to traffic loads in the lower layers of flexible pavements increase. The lower layers of flexible pavements will become more prone to failure because the physical and mechanical properties of the aggregates in these layers hinder the aggregates' ability to withstand high traffic loads. As such, the overall pavement performance may be adversely affected since the

aggregates in the lower layers may be more likely to fail and this may cause flexible pavements to fail prematurely.

In terms of the backcalculated base layer modulus of the pavement sections, Figure 9 reveals several trends. The results in the figure indicate that the cement stabilized base section (Section 3) had the highest backcalculated base layer modulus while the geogrid stabilized base section (section 4) had the lowest backcalculated base layer modulus. The results presented in the figure also indicate that the $CaCl_2$ stabilized base section (Section 2) and bituminous stabilized base section (Section 1) had relatively similar backcalculated base layer moduli values (approximately 37,000 psi (255 N/mm^2) as the untreated base section (control section). These results suggest that Portland cement was the best stabilizing agent to use for stabilizing aggregate base layers, while the geogrid was the least effective stabilizing agent to use for stabilizing aggregate base layers. These results also suggest that the using calcium chloride or bituminous material to stabilize aggregate base layers may have little or no effect in improving the stiffness of aggregate base layers immediately after construction.

Impact of Stabilized Base on the Field Performance of the Pavement Sections

This section presents the results of the layered elastic analysis, which was performed using the backcalculated layer moduli of the pavement sections and Kenpave software. A comparison of the mechanical responses for all sections immediately after construction and at the crack initiation stage is also presented in this section. It is important to reiterate that crack initiation in flexible pavement occurs when the moduli values of the HMA layers are reduced by 50% from their initial values immediately after construction [36].

Impact of stabilized base on pavement section fatigue cracking resistance.

The tensile strains at the bottom of the HMA layer of all pavement sections immediately after construction and at the crack initiation stage are presented in Figure 10 below. Of all the sections analyzed in the study, the Portland cement stabilized base section (i.e., Section 3) had the lowest tensile strains at the bottom of its HMA layer immediately after construction. The tensile strain below the HMA layer of Section 3 immediately after construction was 110 micro-strains. This tensile strain was approximately 56% less than that of the section containing the untreated RAP base (i.e. the control section). The tensile strain below the HMA layer of the section containing the untreated RAP base was 251 micro-strains. These results suggest that the cement stabilized base may have a better fatigue cracking resistance than the untreated base and the other stabilized bases.

The results presented in Figure 10 also indicate that the tensile strains below the HMA layer of the $CaCl_2$ stabilized base section were comparable or similar to those of the untreated base section immediately after construction. The tensile strain below the HMA layer of the $CaCl_2$ stabilized base section was 233 micro-strains. This represented a 7% difference between the tensile strains obtained for the HMA layers of the $CaCl_2$ stabilized base section and the untreated base section. These results indicate that both sections may have the same ability to resist fatigue cracking.

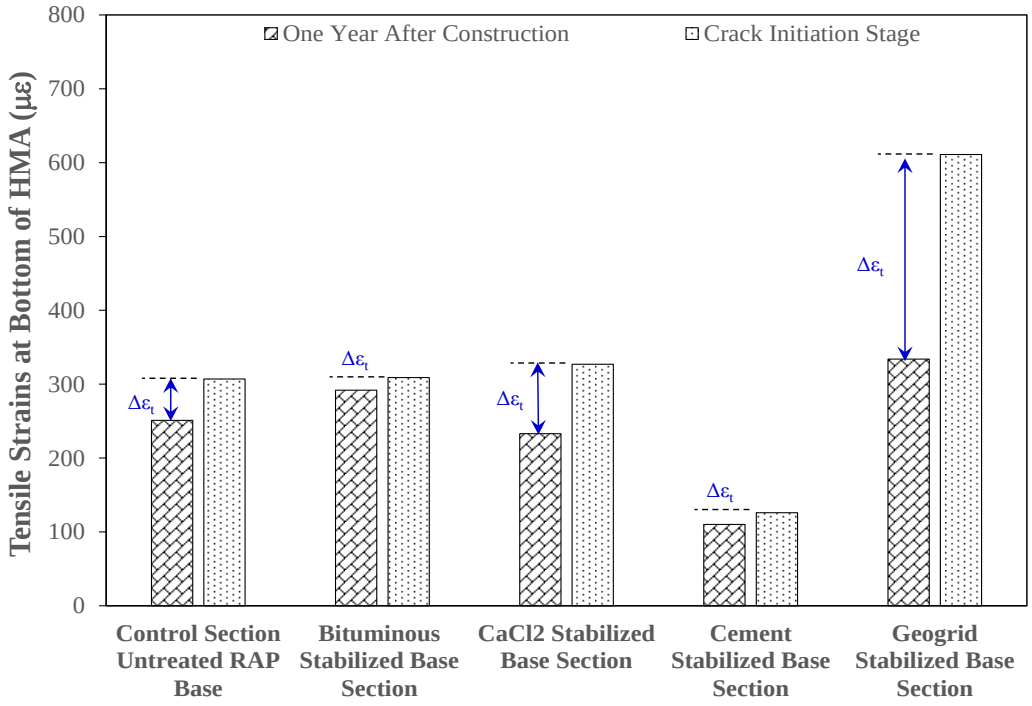

Figure 10. Comparison of tensile strain at the bottom of the HMA layer of all sections one year after construction and at crack initiation

Furthermore, the results in Figure 10 show that Section 4 (i.e., the section containing geogrid) and Section 1 (i.e., the section containing bituminous material) had higher tensile strains than those obtained for the control section immediately after construction. The tensile strain below the HMA layer of Section 4 was 373 micro-strains while that of Section 1 was 321 micro-strains. Therefore the tensile strains obtained for these two pavement sections were approximately 49% and 28% respectively higher than the control untreated base section. This suggests that utilizing geogrid or emulsified asphalt (bituminous material) may have a negative impact on the ability of flexible pavements to resist fatigue cracking.

Moreover, by comparing the difference in tensile strains, $\Delta\varepsilon_t$, obtained immediately after construction and those obtained at the stage of crack initiation, the

impact of the type of stabilized base on the fatigue life of flexible pavements can be determined. As can be seen from Figure 10, the $\Delta\varepsilon_t$ values for the control section were lower (by 18% and 61%) than those obtained for Sections 2 and 4, respectively. This observation indicates that these sections will have a lower fatigue life than the control section since the fatigue life of flexible pavements is characterized by the rate at which a fatigue cracking criterion is met. Sections 2 and 4 are expected to fail faster (in terms of fatigue) than the control section. This is because the increase in tensile strain below the HMA layers of these sections are significantly higher than that of the control section, when all three pavement sections are subjected to the same amount of load repetitions. The results in Figure 10 also show that the $\Delta\varepsilon_t$ for the control section was higher than that obtained for Sections 3 and 1, by approximately 7% and 16% respectively. This suggests that these sections (i.e., Sections 3 and 1) have a longer fatigue life than the control section. Therefore, it can be concluded that sections 3 and 1 will not fail as fast as the control section with respect to fatigue cracking.

Impact of stabilized base on pavement section rutting resistance. The compressive strains at the top of the subgrade layer of all the pavement sections immediately after construction and at the crack initiation stage are presented in Figure 11 below. As can be seen in this figure, the sections containing the geogrid stabilized base and the bituminous stabilized base had similar compressive strain values on top of their respective subgrade layers when compared with that of the control section. The compressive strains at the top of the subgrade layers of the geogrid and bituminous stabilized base sections were 403 micro-strains and 395 micro-strains respectively while the compressive strains obtained for the untreated base section was 406 micro-strains.

These results suggest that both the geogrid and bituminous stabilized base sections had a similar impact as the untreated base section on the rutting susceptibility of the flexible pavement sections. This implies that the stabilization of base layers using geogrid and bituminous material (i.e. emulsified asphalt) may provide minimal benefit in terms of reducing the rutting susceptibility of flexible pavements.

The results presented in Figure 11 also provide insight about the impact of the $CaCl_2$ and cement stabilized base layers on their respective pavement section's ability to resist rutting. The compressive strains on top of the subgrade layer of these two sections immediately after construction were 298 micro-strains (for the $CaCl_2$ stabilized base section) and 267 micro-strains (for the cement stabilized base section). Therefore the compressive strains obtained for the sections containing the $CaCl_2$ and cement stabilized bases were approximately 26% and 34% respectively lower than those obtained for the control section. These results indicate that both the $CaCl_2$ and cement stabilized bases had a positive impact (i.e., improve rutting resistance) on the ability of the entire pavement section to resist rutting.

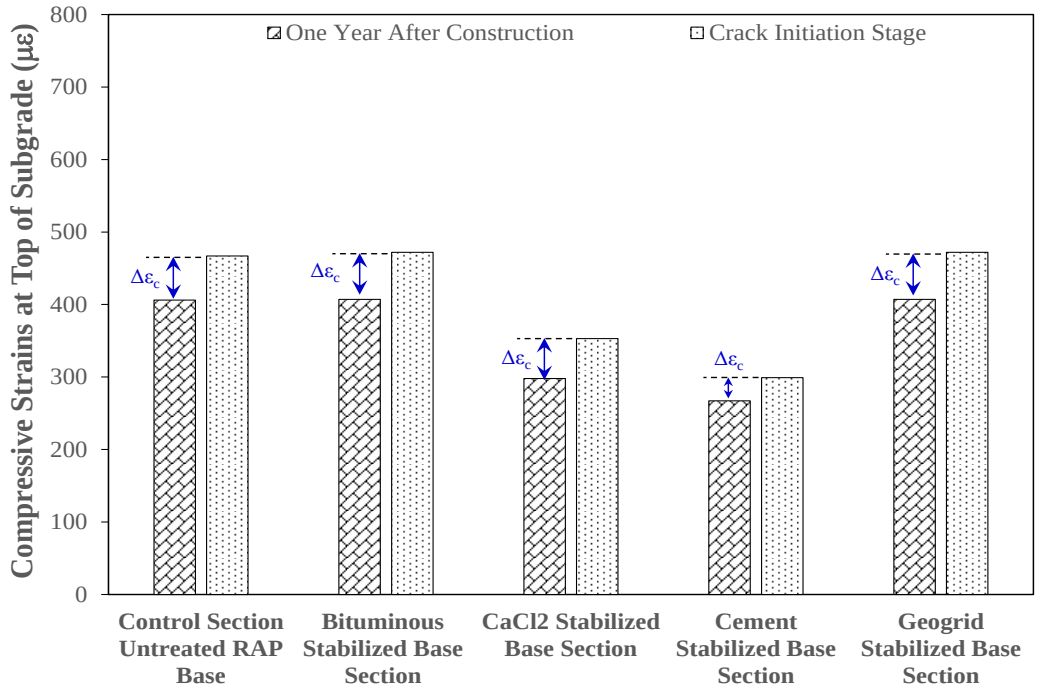

Figure 11. Comparison of compressive strain at the top of the subgrade of all sections immediately after construction and at crack initiation

In the case of the rutting susceptibility, the change in compressive strains ($\Delta\varepsilon_c$) at the top of the subgrade provides insight about the impact of the stabilized bases on the rutting life of the pavement sections. The results illustrated in Figure 11 show that all stabilized base sections had similar $\Delta\varepsilon_c$ values as the untreated (control) base section; with the exception of the cement stabilized base section. This suggests that all the stabilized sections except the cement treated section will fail, in terms of rutting, after the same amount of time. With respect to the cement treated section, the $\Delta\varepsilon_c$ approximately 48% lower than the $\Delta\varepsilon_c$ of the untreated section. The $\Delta\varepsilon_c$ of the cement treated section was 32 micro-strains while that of the untreated base section was 61 micro-strains. These results imply that using a cement treated base layer in flexible pavements improves the rutting life (i.e. performance) of the overall pavement structure.

Pavement ME Design Predicted Performance

This section presents the results of the Pavement ME design simulations. The total predicted fatigue cracking and rutting in each of the pavement sections are discussed in addition to implications of the results of the design simulations on the overall performance of the pavement sections.

Pavement ME total predicted fatigue cracking. The results of the predicted fatigue cracking are illustrated in Figure 12 below. As can be seen in this figure, the total predicted of fatigue cracking in the sections containing the $CaCl_2$ stabilized base and bituminous stabilized base was relatively similar to the predicted fatigue cracking in the control section. The total predicted fatigue cracking in the control section was approximately 1,650 ft./mile (312.5 m/km) while the total predicted fatigue cracking in the $CaCl_2$ stabilized base and bituminous stabilized base was 1,825 ft./mile (345.6 m/km) and 1,865 ft./mile (353.2 m/km) respectively. These results confirm the trend observed in the layered elastic analysis results as they indicate that $CaCl_2$ and bituminous stabilized base sections have relatively the same susceptibility to fatigue cracking as the untreated base section.

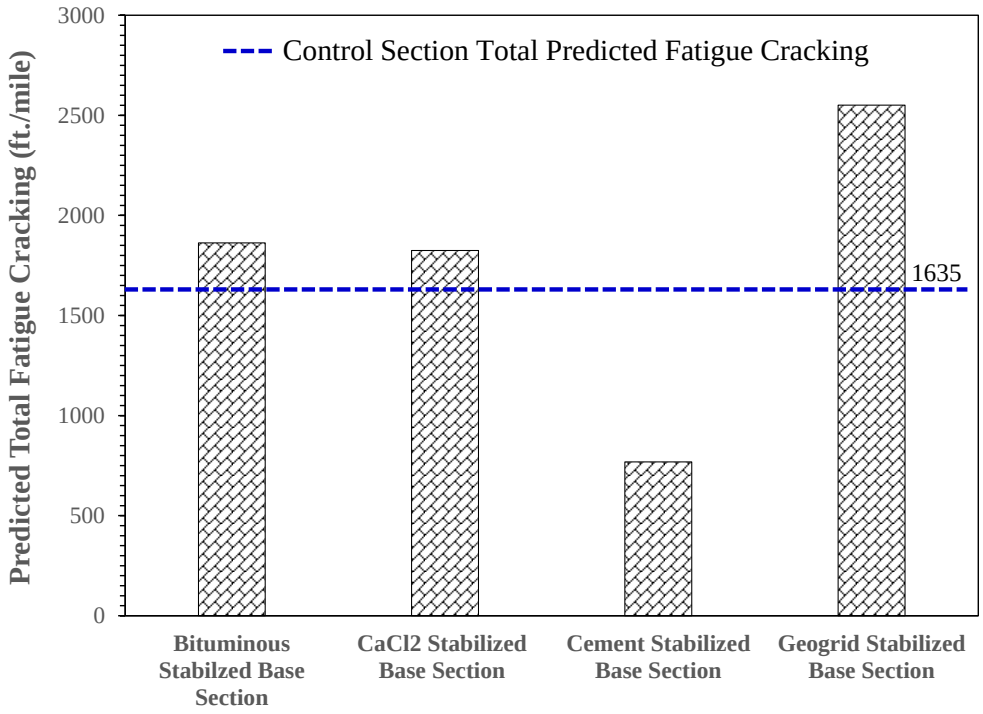

Figure 12. Total predicted fatigue cracking in pavement sections

The results illustrated in Figure 12 also show that Section 3, which contained the cement treated base layer, had lower total predicted fatigue cracking values than the control section. The total predicted fatigue cracking of this section (i.e. Section 3) was 769 ft./mile (145.6 m/km); which was approximately 53% lower than that of the control section. This observation implies that the use of cement treated bases improves the fatigue life of flexible pavements. With respect to the predicted fatigue cracking in the geogrid stabilized base section (i.e. Section 4), the results in Figure 12 indicate that this pavement section may be more susceptible to fatigue cracking than the control section. This is believed to be the case because the total predicted fatigue cracking in Section 4 was 2,551 ft./mile (483 m/km); which was substantially higher (i.e., 56%) than that obtained for the control section.

Pavement ME total predicted rutting. The values of the total predicted rutting for all pavement sections analyzed with Pavement ME are presented in Figure 13 below. As can be seen from this figure, the total predicted rutting, after 20 years of traffic loads, for the control section as well as Sections 1 2, and 3 was similar. The total predicted rutting of both Sections 1, and 2 (i.e. the bituminous stabilized, and $CalCl_2$ stabilized base sections respectively) was 0.3 in. (7.62 mm) while those of Section 3 (i.e. the cement stabilized base section) and the control section were 0.27 in. (6.85 mm) and 0.3 in. (7.62 mm) respectively. These results indicate that the rutting susceptibility, as predicted using Pavement ME Design, was similar for the control section and Sections 1, 2, and 3.

With regard to the total predicted rutting for section 4 (i.e. the section containing the geogrid stabilized base), the results in Figure 13 indicate that predicted rutting in this section was 0.37 in. (9.40 mm). This total predicted rutting was higher (by about 23%) than the total predicted rutting obtained for the control section. This suggests that using geogrid to stabilize aggregate base layers may have a negative impact on flexible pavements' rutting life, which supports the results of the layered elastic analysis.

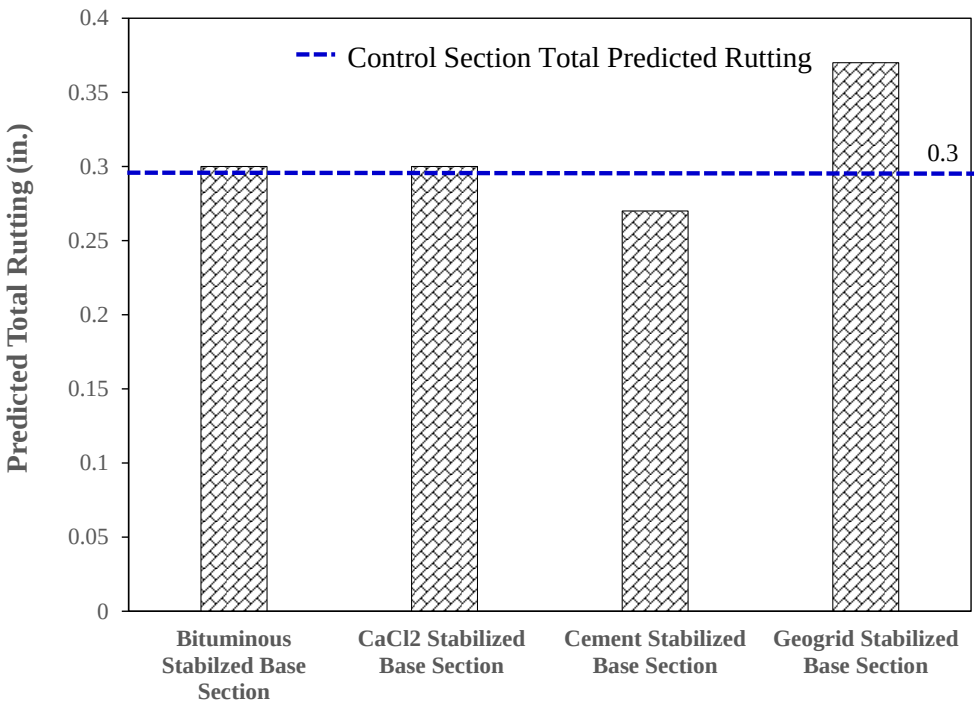

Figure 13. Total predicted rutting in pavement sections

Determining Change in Pavement Condition with Time using PSHI

This section presents a comparison of the change in pavement condition of all the pavement sections with time. The results of the Pavement ME design simulations are used in conjunction with the RIDOT Pavement Structural Health Index (PSHI) to determine the change in condition of each of the pavement sections. The Pavement Structural Health Index is a tool used to assess and monitor the condition of flexible pavements. It is a weighted average that is determined from a comprehensive scoring system which accounts for flexible pavement distresses such as International Roughness Index (IRI), rutting, cracking (i.e. longitudinal, transverse, alligator, and block), and patch failure [38]. The weight distribution of the pavement distresses accounted for in the RIDOT PSHI scoring system are presented in Table 5 below.

Table 5

RIDOT Pavement Structural Health Index scoring system weight distribution

Pavement Distress	Weight Distribution of Distress Scores in RIDOT PSHI Scoring System
Alligator Cracking	16
Longitudinal Cracking	7
Transverse Cracking	7
Block Cracking	10
Patch Failure	20
Total Rutting	10
International Roughness Index (IRI)	30

The pavement distress which are factored into the overall RIDOT PSHI scoring system each have their respective scoring systems. The scores in these individual pavement distress scoring systems typically range from 0 to 100 and they are determined based on a 328 ft. (100 m) long test section of a roadway [32]. The scoring system for alligator cracking, longitudinal cracking and transverse cracking are presented in Table 6 below. The scores designated in the respective scoring systems for each type of cracking depend on whether the amount of cracking falls within a particular range. The general trend in the scoring system for each type of cracking indicate that the score increases as the amount of alligator, longitudinal, and transverse cracking decrease respectively.

Table 6

RIDOT scoring system for alligator, longitudinal and transverse cracking on flexible pavements

Alligator Cracking		**Longitudinal Cracking**		**Transverse Cracking**	
Ranges ($ft.^2$)	**Score**	**Ranges ($ft.^2$)**	**Score**	**Ranges (ft./mi)**	**Score**
0 – 10.8	100	0 – 10.8	100	0 – 57.0	100
10.8 - 322.9	90	10.8 - 322.9	90	57.0 – 170.5	95
322.9 - 645.8	80	322.9 - 645.8	80	170.5 – 284.0	90
645.8 – 968.8	70	645.8 – 968.8	70	284.0 – 397.6	85
968.8 - 1291.7	60	968.8 - 1291.7	60	397.6 – 511.6	80
1291.7 - 1614.6	50	1291.7 - 1614.6	50	511.6 – 625.2	75
1614.6 - 1937.5	40	1614.6 - 1937.5	40	625.2 – 739.2	70
1937.5 - 2260.4	30	1937.5 - 2260.4	30	739.2 – 852.7	65
2260.4 - 2583.3	20	2260.4 - 2583.3	20	852.7– 966.2	60
2583.3 - 2906.3	10	2583.3 - 2906.3	10	966.2– 1079.8	55
2906.3 <	0	2906.3 <	0	1079.8 – 1193.2	50

The scoring system for rutting is presented in Figure 14 below [38]. The scoring system for rutting generally becomes stricter once the total rutting on a flexible pavement exceeds 1in. (25.4 mm). As the total rutting reaches and exceeds 1.5 in. (38.1 mm), the rutting score becomes 0. It is important to note that he graph in Figure 14 does not extend all the way to 100 because a rutting score of 100 is assigned to pavements which experience less than 0.28 in. (7.1 mm) of rutting [32]. The scoring system for IRI is presented in Figure 15. From this figure, it can be observed that an IRI score of 100 is assigned to a flexible pavements which have an IRI of 75 in./mile (1.2m/km) or less. It can also be seen from the figure that an IRI score of 0 is allocated to flexible pavements which have an IRI of 400 inches/mile (6.3 m/km) or more.

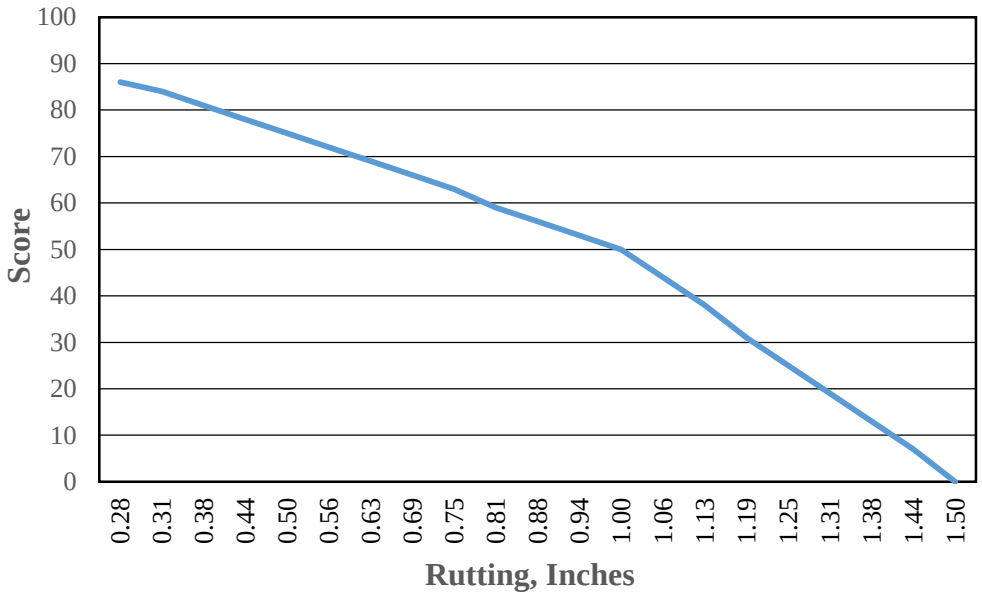

Figure 14. RIDOT rutting distress scoring system for flexible pavements

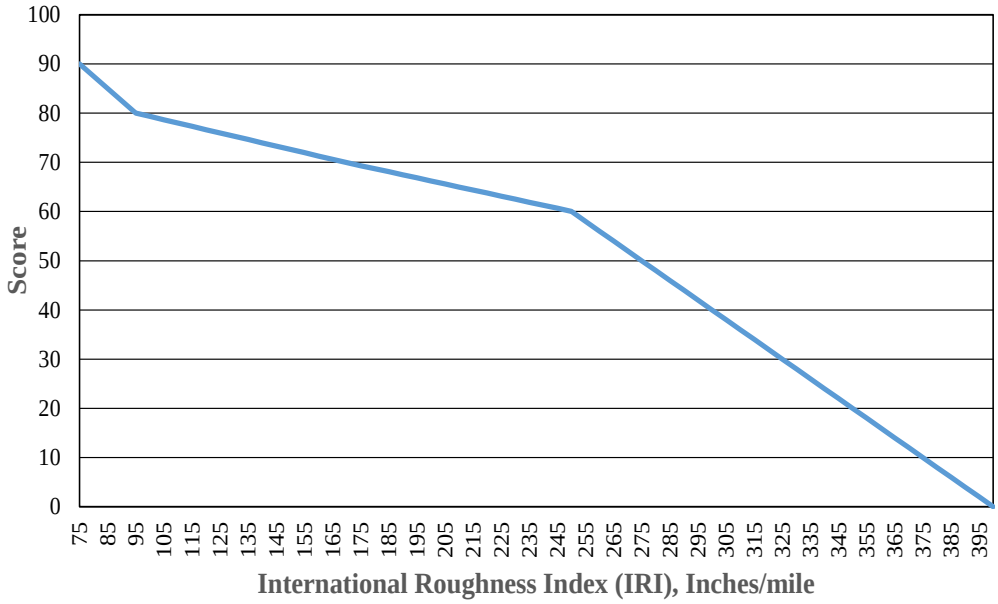

Figure 15. RIDOT IRI distress scoring system for flexible pavements

The overall PSHI score of flexible pavements is generally used to qualitatively classify the condition of the pavement as excellent, good, fair, poor, or failed. These classifications for pavement condition depend on whether the overall PSHI score of a flexible pavement falls within a particular range of values. The scores for the overall PSHI of flexible pavements typically range from 0 to 100. However, the range of the overall PSHI score for the pavement sections evaluated in the study had to be modified to 0 to 70 because the scope of the study did not account for block cracking and patch failure in flexible pavements. Therefore the final PSHI scores of the pavement sections analyzed in the study were calculated as percentages; with 70 being the total or maximum PSHI score. It is important to note that the pavement condition was classified as excellent when the PSHI scores of the pavement sections fell within the 90.5 to 100 range. Additionally, the pavement condition was classified as good, fair, poor, and failed when the PSHI score fell within 84.1 to 90.5 range, 75.6 to 84.1 range, 64.5 to 75.6 range, and 0 to 64.5 range respectively [38].

Evaluation of pavement section condition. Figure 16 below presents the change in PSHI score of each pavement section (i.e. the control section and the sections containing the stabilized bases) during the 20 year Pavement ME analysis period. The threshold PSHI score for pavement serviceability used by RIDOT is also shown in the Figure 16. The threshold PSHI score for pavement serviceability was 64.5 because this score was the upper limit for the range of PSHI scores that represented a "failed" pavement condition. It can be observed in Figure 16 that the section containing the cement stabilized base had the smallest reduction in PSHI score as trafficking progressed on the pavement section during the analysis period. The PSHI score of the cement

stabilized section decreased from 100 to 78.4. Quantitatively this reflected a 21.6% decrease in PSHI score and indicated that the condition of the cement stabilized section deteriorated from an excellent condition to a fair condition after 20 years of trafficking.

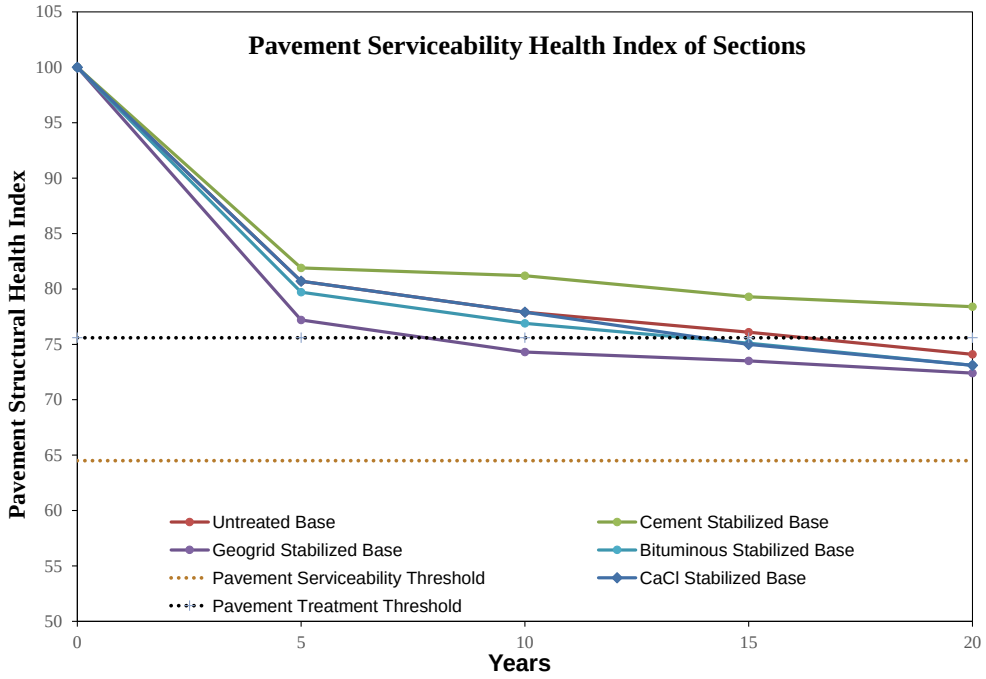

Figure 16. Change in Pavement Structural Health Index of pavement sections with time

In regard to the sections containing the calcium chloride stabilized base and bituminous stabilized base, the PSHI score decreased from 100 to 73.1 on both sections after 20 years of trafficking. This reflected a 26.9 % reduction in PSHI score and indicated that the pavement condition of both pavement sections declined from excellent to poor during the 20-year Pavement ME analysis period. The section containing the untreated RAP base experienced a decrease in PSHI score from 100 to 74.1 during the 20 year analysis period and this reflected a 25.9% reduction in PSHI score. Qualitatively,

this meant that the condition of this section declined from excellent to poor after the pavement section was subjected to 20 year of trafficking. With respect to the section containing the geogrid stabilized base, the PSHI score declined from 100 to 72.4 during the pavement ME analysis period. This reflected a 27.6% decrease in PSHI score and a change in pavement condition from excellent to poor.

Comparison of pavement section condition over time. It can be observed in Figure 16 that none pavement sections containing the stabilized/untreated base layers experienced a "failed" pavement condition during the 20 year Pavement ME analysis period. However, the PSHI score of all the pavement sections (except the Portland cement stabilized base section) met the pavement treatment threshold during this period. The time required for the PSHI score of the pavement sections to reach the pavement treatment threshold can be used to compare the impact of the base layer stabilization on pavement condition. This change in PSHI score reflected a decline in pavement condition from excellent to poor.

Figure 16 above, shows that the PSHI score on the control section (i.e. the section containing the untreated RAP base) reached the pavement treatment threshold after the pavement section experienced 16.25 years of trafficking. This figure also indicates that the PSHI score of the cement stabilized base section, did not reach the pavement treat threshold during the 20 year analysis period. With respect to the sections containing the $CaCl_2$ and bituminous stabilized bases, the PSHI score on both sections reached the pavement treatment threshold after 14 years and 13.4 years respectively. This indicated the pavement condition of the $CaCl_2$ and bituminous stabilized base sections declined at a relatively similar rate to that of the control section. In regard to the section containing the

geogrid stabilized base, the PSHI score of the pavement section reached the pavement treatment threshold after 7.8 years of trafficking. This implied that the condition of the pavement on the geogrid stabilized section deteriorated at approximately twice the rate of the control section.

Comparison of Life Cycle Costs of Pavement Sections

The life cycle costs of the pavement sections gives insight about the cost effectiveness of conducting full depth reclamations of flexible pavements using the stabilizers considered in this study. The life cycle costs of the pavement sections can be determined from the change in the pavement section condition over time. A major component of the life cycle costs of the pavement sections evaluated in the study is the rehabilitation costs of the respective sections. The rehabilitation costs of the pavement sections can be determined from the time required for the PSHI score of the pavement sections to reach the pavement preservation threshold (i.e. transition of pavement condition from excellent to poor). Generally when this occurs, an intervention is made in order to preserve the pavement. These intervention usually involve the application of treatments to the surface layers of flexible pavements.

In Rhode Island several treatments are typically applied to the surface layers of flexible pavements in order to preserve the pavements. These treatments include: Stress Absorbing Membrane interlayer (SAMI), crack seal, mill and overlay, Paver Placed Elastomeric Surface Treatment (PPEST), and rubberized chip seal [32]. For the purpose of this study, mill and overlay was selected as the treatment which should be applied when the condition of the pavement sections became "poor." This is because the mill and overlay

treatments usually maintains pavement serviceability for a longer period (5 to 10 years) than the other treatment options [32]. In the study, the worst case scenario was used to determine rehabilitation costs in which mill and overlay treatment was assumed to only add 5 years of pavement serviceability. It is important to note that the average cost of conducting a mill and overlay of the pavement sections was approximately $142,000 per lane mile [32]. The total rehabilitation costs of the pavement sections was found by determining the amount of treatment interventions required on the pavement sections during the 20 year Pavement ME analysis period and multiplying that number by the cost of conducting a mill and overlay.

The surface layer of the control section required a mill and overlay once during the analysis period. As a result the total rehabilitation cost of this section was $142,000 per lane mile. The pavement section which required the most treatment interventions during the 20 year analysis period was the geogrid stabilized base section. This pavement section required a mill and overlay during the 8th year, 13th year, and 18th year of the analysis period. An initial mill and overlay was required near the end of the 8th year in the analysis period because the condition of this pavement section transitioned from fair to poor during this period. Two additional mill and overlays were required during the 20 year analysis period because the mill and overlay was assumed to only add 5 years of pavement serviceability. As such, the total rehabilitation cost of this section was determined as $426,000 per lane mile. The bituminous stabilized and $CaCl_2$ stabilized sections both had a total rehabilitation cost of $284,000 per lane mile because these two sections required two treatment interventions during the analysis period. A mill and overlay was required on both pavement sections during the 14th and 19th year of the analysis period. The

rehabilitation cost of the Portland cement stabilized section was $0 per lane mile since this section did not require treatment for the entire 20 year period.

In addition to the rehabilitation costs, the initial cost of constructing the pavement sections was also factored into the life cycle costs of the pavement sections. Table 7 below, presents the initial costs of constructing the pavement sections analyzed in this study. The initial cost of constructing the pavement sections was determined by adding the construction costs of the full depth reclamations and the cost of constructing the HMA, subbase, and subgrade layers. The cost of constructing the HMA layers, on each pavement section was $3,589,780 per lane mile while the cost of constructing the in-situ (subbase and subgrade) layers was 88,967 per lane mile. From Table 7, it can be seen that the pavement section with the highest initial construction costs was the cement stabilized base section while the pavement section with lowest initial construction cost was the section containing the untreated RAP base.

Table 7

Initial construction costs of untreated and stabilized pavement sections [38]

Pavement Section	**Initial cost of constructing the pavement sections ($) per lane mile**
(Control) Untreated base	3,693,572
Bituminous stabilized base	3,775,547
$CaCl_2$ stabilized base	3,798,132
Cement stabilized base	4,024,155
Geogrid stabilized base	3,884,247

Note. All costs are rounded to the nearest dollar.

The total life cycle cost for each section is presented in Table 8 below. The total life cycle cost of the pavement sections was determined by adding the initial construction costs of the pavement sections to their respective rehabilitation costs for the 20 year analysis period. The results presented in Table 8 indicate the section containing the geogrid stabilized base had the highest life cycle cost while the control section had the lowest life cycle cost. The results in this table also show that the pavement sections containing the bituminous stabilized base, $CaCl_2$ stabilized base and Portland cement stabilized base all had relatively similar lifecycle costs (approximately $4,000,000 per lane mile). Overall the results of the life cycle cost analysis of the pavement sections reveals that it may not be cost effective to use bases stabilized by asphalt emulsions, $CaCl_2$, Portland cement, and geogrids in flexible pavement sections on RI Route 165. However it is important to note that the results of the lifecycle cost analysis is based on the predicted performance of the pavement sections. Therefore definite conclusions can be made about the cost effectiveness constructing flexible pavements with stabilized bases.

Table 8

Total life cycle costs of the pavement sections containing the stabilized and untreated base layers

Pavement Section	Total life cycle cost pavement sections ($) per lane mile
(Control) Untreated base	3,835,572
Bituminous stabilized base	4,059,547
$CaCl_2$ stabilized base	4,082,132
Cement stabilized base	4,024,155
Geogrid stabilized base	4,310,247

Note. All costs are rounded to the nearest dollar.

Chapter 5

Summary of Findings, Conclusions & Recommendations

Summary of Findings

The research presented in this study evaluated the impact of stabilized and untreated base layers on field performance (i.e., fatigue and rutting) of flexible pavements. Five field sections located on Route 165 (between utility poles 304 and 521) in Rhode Island were evaluated. These sections are part of a controlled study currently being conducted by RIDOT to evaluate their long-term field performance. Four of the five sections were constructed using stabilized base layers and one was constructed as a control section using untreated RAP aggregates. The approach utilized to evaluate the impact of different stabilizing agents (or stabilized bases) on field performance of flexible pavements involved conducting FWD tests on all selected field sections. The collected FWD data (or deflections) were used to backcalculate the elastic moduli for all layers in each pavement section. The influence of the stabilized bases and the untreated control RAP base on the mechanical responses (i.e. stresses and strains) of the overall pavement structure was also evaluated by conducting layered elastic analyses. In addition, AASHTOWare Pavement ME Design simulations were conducted to determine which of the four stabilized base types enhanced the overall performance of flexible pavements the most. The results of the Pavement ME Design simulations were then used to analyze the life cycle costs of each pavement section in order to determine the most cost effective stabilized base.

The results of the layered elastic analysis provided insight about the fatigue cracking and rutting susceptibility of the pavement sections considered in the study. The fatigue and rutting lives of the pavements were also determined from the layered elastic analysis. The results of the layered elastic analysis were as follows:

- The field section containing an untreated RAP base had a tensile strain of 251 micro-strains at the bottom of the HMA layers immediately after construction. The field sections containing a $CaCl_2$ stabilized base, cement stabilized base, geogrid stabilized base and bituminous stabilized had tensile strains of 233 micro-strains, 110 micro-strains, 373 micro-strains and 321 micro-strains at the bottom of their respective HMA layers immediately after construction.
- The change in tensile strain ($\Delta\varepsilon_t$) below the HMA layers of the field sections containing the $CaCl_2$ stabilized base and the geogrid stabilized base was 18% and 61% respectively, higher than that of the control section at crack initiation. The $\Delta\varepsilon_t$ below the HMA layers of the cement stabilized and bituminous stabilized base sections was 7% and 16% respectively lower than that of the control section at crack initiation.
- The field section containing an untreated RAP base had a compressive strain of 406 micro-strains at the top of the subgrade layer immediately after construction. The field sections containing a $CaCl_2$ stabilized base, cement stabilized base, geogrid stabilized base and bituminous stabilized base had compressive strains of 298 micro-strains, 267 micro-strains, 403 micro-strains and 395 micro-strains at the bottom of their respective HMA layers immediately after construction.

- The change in compressive strain ($\Delta\varepsilon_c$) on top the subgrade layer of all the field sections except the cement stabilized base section was approximately 61 micro strains at crack initiation. The $\Delta\varepsilon_c$ on the field section containing the cement-stabilized base was 18% lower than that of the control section since the $\Delta\varepsilon_c$ on the cement stabilized section was 32 micro-strains at crack initiation.

The results of the Pavement ME predicted performance also provided insight about the fatigue cracking and rutting susceptibility of the pavement sections considered in the study. The results of the Pavement ME design simulations were as follows:

- The predicted fatigue cracking on the field section containing an untreated RAP base was 1650 ft./mi (312.5 m/km) after the pavement section experienced 20 years of traffic. The predicted fatigue cracking of the field sections containing a $CaCl_2$ stabilized base, cement stabilized base, geogrid stabilized base and bituminous stabilized base was 1825 ft./mi (345.6 m/km), 769 ft./mi (145.6 m/km), 2551 ft./mi (483 m/km), and 1865 ft./mi (353.2 m/km) respectively after the pavement sections were subjected to 20 years of traffic.
- The predicted rutting on the field sections containing an untreated RAP base, $CaCl_2$ stabilized base, and bituminous stabilized base was 0.3 in. (7.62 mm) after the pavement section experienced 20 years of traffic. The predicted rutting on the field section containing a cement stabilized base was 0.27 in. (6.25 mm) while that of the section containing the geogrid stabilized base was 0.37 in. (9.40 mm) when both pavement sections were subjected to 20 years of traffic.

The life cycle costs of the pavement sections were determined by analyzing the construction and rehabilitation costs of the five field sections as well as the change in Pavement Structural Health Index (PSHI) during the Pavement ME analysis period. The results of the Pavement ME predicted performance were used to determine the PSHI of the pavement sections in order to investigate the change in pavement condition of the pavement sections during the Pavement ME analysis period. The results of the life cycle cost analysis were as follows:

- The life cycle costs in, per lane mile, of the field sections containing untreated RAP base, bituminous stabilized base, $CaCl_2$ stabilized base, Portland cement stabilized base, and geogrid stabilized base was \$3,.83 M, \$4,.05 M, \$4,.08 M, \$4,.02 M, and \$4,.31 M , respectively.

Conclusions

Based on the results of the layered elastic analysis and Pavement ME performance predictions obtained for the pavement sections considered in the study, the following conclusions can be drawn:

- The Portland cement treated base appeared to be more effective than the other stabilized bases at extending the predicted fatigue life of the flexible pavement sections. The Portland cement treated base also appeared to reduce the susceptibility of the pavement section to fatigue cracking more than the other stabilized bases.
- The $CaCl_2$ stabilized and bituminous stabilized bases seemed to have a similar impact as the control (untreated RAP base) on the overall predicted fatigue

performance of the flexible pavement sections. However, only the bituminous stabilized base appeared to have a similar impact as the control base (untreated RAP base) on the fatigue cracking potential of the overall pavement.

- The geogrid stabilized base seemed to have the lowest impact on the predicted fatigue and rutting lives of the overall pavement. The geogrid stabilized base also appeared to have the lowest impact in terms of reducing the susceptibility of the overall pavement section to fatigue cracking. It is important to note however, that the effect and strength of the geogrid could not be fully captured by the impulse load applied during FWD testing. This was a shortcoming which arose due to the scope of the scope of this study.
- Base layer stabilization may not have a significant impact on the overall rutting performance of flexible pavements because the predicted rutting performance of all the pavement sections were similar.
- It may not be cost effective to use stabilized bases (i.e. bases stabilized with by asphalt emulsions, $CaCl_2$, Portland cement, and geogrids) in flexible pavement sections on RI Route 165 since the lifecycle cost of the untreated RAP base section appeared to be the lowest of all the pavement sections analyzed in the study. It is important to note however that the lifecycle cost of the pavement sections were evaluated based on the predicted performance of the pavement sections. Hence no definite conclusion can be made about the cost effectiveness of base layer stabilization.

Recommendations

The following recommendations can be made about using the stabilized bases considered in this study in flexible pavements:

- Portland cement may be used as a stabilizing agent in the base layer of flexible pavements. This is because it appeared to have the greatest impact on the predicted fatigue life of the flexible pavement section.
- Calcium chloride and asphalt emulsions may not be feasible stabilizing agents for the base layers of flexible pavements because they appeared to have no significant impact on the predicted fatigue performance. Additionally the lifecycle costs of flexible pavements containing these bases seemed to be higher when compared to untreated RAP bases.
- Geogrids are may be the least effective stabilizing agents to use in the base layers of flexible pavements because it seemed to have the lowest impact on the predicted fatigue cracking of flexible pavement sections. However, due to the limitations of testing carried out in this study, no evidence is provided to conclusively state that geogrids are ineffective base layer stabilizing agents.

References

[1] Y. H. Huang, "Stresses and Strains in Flexible Pavements" in *Pavement Analysis and Design*, 2nd ed. Upper Saddle River, NJ, 2004, ch.2, sec.2.2, pp.57-76.

[2] E. Tutumluer, "Practices for Unbound Aggregate Pavement Layers: A Synthesis of Highway Practice." Transportation Research Board of the National Academies, Washington, D.C., Rep. NCHRP Synthesis 445, 2013.

[3] W. Kipp et al., "Reclaimed Base Course Stabilized with Calcium Chloride," Materials and Research Section, State of Vermont Agency of Transportation, Montpelier, VT, Rep. 2008-4, 2008.

[4] S. Tang et al., "Structural Evaluation of Asphalt Pavements with Full-Depth Reclaimed Base," Minnesota Department of Transportation Research Services, St. Paul, MN Rep. MN/RC 2012-36, 2012.

[5] S. Sebsta and T. Scullion, "Effectiveness of Minimizing Reflective Cracking in Cement-Treated Bases by Microcracking," Texas Department of Transportation Research and Technology Implementation Office, Austin, TX, Rep. FHWA/TX-05/0-4502-1, 2004.

[6] S. Sebesta, "Test Use of Microcracking to Reduce Shrinkage Cracking in Cement Treated Bases," *Transportation Research Record: Journal of the Transportation Research Board*, vol. 1936, pp.1-11, Jan., 2005.

[7] H.E. Bofinger et al., "The Shrinkage of Fine-Grained Soil-Cement," Transport and Road Research Laboratory, Crawthorne, England, Rep. 398, 1978.

[8] J.G. Zornberg and R. Gupta, "Geosynthetics in pavements: North American Contributions," *9th International Conference of G*eosynthetics, Guaruja, Brazil, 2010, pp.379-398.

[9] O. Ogundipe, "Strength and Compaction Characteristics of Bitumen-Stabilized Granular Soil," *International Journal of Scientific & Technology Research,* vol. 3, no. 9, Sep. 2014.

[10] S. Khosravifar, and C. Schwartz, "Design and Evaluation of Foamed Asphalt Base Materials," Maryland State Highway Administration Office of Policy and Research, Maryland State Highway Administration, Baltimore, MD, Rep. MD-13-SP909B4E, 2013.

[11] D. Saylak et al., "Fly Ash-Calcium Chloride Stabilization in Road Construction," *Transportation Research Record: Journal of the Transportation Research Board,* vol. 2053, pp.23-29, Dec., 2008.

[12] D. Saylak et al., "Base Stabilization and Dust Control Using calcium Chloride and Fly Ash," in *International Ash Utilization Symposium*, Lexington, KY, 2003.

[13] H. Kirchner and J. A. Gail. "Liquid Calcium Chloride Dust Control and Base Stabilization of Unpaved Road Systems," *Transportation Research Record: Journal of the Transportation Research Board*, vol. 1291, pp.173-178, Aug., 1991.

[14] C. Shon et al., "Combined Use of Calcium Chloride and Fly Ash in Road Base Stabilization," *Transportation Research Record: Journal of the Transportation Research Board*, vol. 2186, pp.120-129, Dec., 2010.

[15] W. Grogan et al., "Stabilized Base Coaurses for Advanced Pavement Design Report 1: Literature Review and Field Performance Data," U.S. Department of Transportation Federal Aviation Administration, Washington, D.C., Rep. DOT/FAA/AR-97/65, 1999.

[16] H. J. Pendola et al., "Evaluation of Factors Affecting the Tensile Properties of Cement–Treated Materials," U.S Department of Transportation, Federal Highway Administration Bureau of Public Roads, Washington, D.C., Rep. 98-3, 1969.

[17] D. Jones et al., "Comparison of Full-Depth reclamation with Portland Cement and Full Depth reclamation with No Stabilizer in Accelerated Loading Test," *Transportation Research Record: Journal of the Transportation Research Board*, vol. 2524, pp.133-142, Jan., 2015.

[18] Y. Wang et al., "Shrinkage Performance of Cement-Treated Macadam Base Materials," *7th International Conference on Traffic and Transportation Studies*, Kunming, China, 2010, pp.1378-1386.

[19] S. P. Singh et al., "Performance Evaluation of Cement Stabilized Fly Ash-GBFS Mixes as a Highway Construction Material," *Waste management*, vol. 28, no. 8, pp.1331-1337, Nov., 2008.

[20] R. Taha et al., "Cement Stabilization of Reclaimed Asphalt Pavement Aggregate for Road Bases and Subbases," *Journal of Materials in Civil Engineering*, vol. 14, no. 3, June, 2002.

[21] S. M. Mounes et al., "Improving Rutting Resistance of Pavement Structures Using Geosynthetics: An Overview," *The Scientific World Journal*, vol. 2014, no. 764218, Jan., 2014.

[22] M. Y. Abu-Farsakh et al., "Evaluation of Geogrid Base Reinforcement in Flexible Pavements using Cyclic Plate Load Testing," *International Journal of Pavement Engineering*, vol. 12, no. 3, pp.275-288, June, 2011.

[23] H. Wu et al., "Evaluation of Geogrid Base Reinforcement on Unbound Granular Pavement Base Courses using Loaded Wheel Tester," *Goetextiles and Geomembranes*, vol. 43, no. 5, pp.462-469, Oct., 2015.

[24] *Cold Recycling: Wirtgen Cold Recycling Technology*, 1st ed., Wirtgen GmbH, Windhagen, Germany, 2010, pp. 73-98.

[25] Z. Wu et al., "Accelerated Pavement Testing on Foamed Asphalt Base Materials," unpublished.

[26] B. Lane et al., "Long Term Performance of Full Depth Reclamation with Expanded Asphalt on the Trans-Canada Highway Near Wawa, Ontario," *2012 Conference and Exhibition of the Transportation Association of Canada-Transportation: Innovations and Oportunities*, New Brunswick, Canada, 2012, pp.12.

[27] Y. Mehta and R. Roque, "Evaluation of FWD Data for Determination of Layer Moduli of Pavements," *Journal of Materials in Civil Engineering*, vol. 15, no. 1, pp. 25-31, Feb., 2003.

[28] P. Donovan and E. Tutumluer, "Falling Weight Deflectometer Testing to Determine Relative Damage in Asphalt Pavement Unbound Aggregate Layers," *Transportation Research Record: Journal of the Transportation Research Board*, vol. 2104, pp.12-23, Dec., 2009.

[29] J. M. Maestas, and M.S. Mamlouk, "Comparison of Pavement Deflection Analysis Methods Using Overlay Design," *Transportation Research Record: Journal of the Transportation Research Board*, vol. 1377, pp.17-21, Aug., 1992.

[30] C. Asil et al., "Backcalculation of Elastic Modulus of Soil and Subgrade from Portable Falling Weight Deflectometer Measurements," *Engineering Structures*, vol. 34, pp. 1-7, Nov. 2011.

[31] Y. H. Huang, "KENLAYER Computer Program," in *Pavement Analysis and Design*, 2nd ed. Upper Saddle River, NJ, 2004, ch.3, sec.3.2, pp.106-108.

[32] S. Coffey, "Developing Pavement Preservation and Mitigation Strategies using Pavement ME Design Guide for Rhode Island DOT," M.S. thesis, Department of Civil and Environmental Engineering, Rowan University, Glassboro, NJ, 2013.

[33] K. Wilson, "Evaluation of Pavement Rehabilitation Strategies on Route 165 and Prediction Performance," Ph.D. dissertation, Department of Civil and Environmental Engineering, University of Rhode Island, Kingston, RI, 2016.

[34] A. V. Brown, "Cement Stabilization of Aggregate Base Materials Blended with Reclaimed Asphalt Pavement," M.S. thesis, Department of Civil and Environmental Engineering, Brigham Young University, Provo, U.T., 2006.

[35] T. A. Redles et al., "Estimating Fatigue Endurance Limits of Flexible Airfield Pavements," *Transportation Research Board 94th Annual Meeting*, Washington, D.C., 2015, pp. 17.

[36] S. Shen and S. Carpenter. "Dissipated Energy Concepts for HMA Performance: Fatigue and Healing," Federal Aviation Administration (FAA), Washington, D.C., Rep. DOT 05-C-AT-UIUC-COE, 2007.

[37] A. Bradshaw et al., "Resilient Moduli of Reclaimed Asphalt Pavement Aggregate Subbase Blends". *Journal of Materials in Civil Engineering*, vol. 28, no. 5, May, 2016.

[38] Y. Mehta. (2016, Oct. 5th). *Fwd:Data* [email].

Appendix

Pavement Deflections

Table A.1

Falling Weight Deflectometer data obtained from pavement section containing the $CaCl_2$ stabilized.

Direction	Distance (ft.)	Impact Load (lbs)	Deflections (mils)						
			D_0	D_1	D_2	D_3	D_4	D_5	D_6
Westbound	858	12,458	15.68	11.29	9.24	5.86	4.00	2.88	2.24
Westbound	2,586	12,342	14.57	9.83	7.81	4.87	3.32	2.39	1.79
Westbound	4,255	12,467	13.25	8.57	6.64	3.69	2.37	1.64	1.26
Westbound	5,946	12,317	14.68	9.52	7.36	4.24	2.95	2.22	1.74
Westbound	7,647	12,285	16.82	10.84	8.57	5.35	3.71	3.45	1.96
Eastbound	887	12,263	16.04	10.36	8.27	5.15	3.51	2.51	1.92
Eastbound	2,569	12,227	16.25	11.05	8.26	4.11	2.56	1.69	1.18
Eastbound	5,866	12,257	14.46	8.85	6.93	3.81	2.34	1.53	1.09
Eastbound	7,987	12,278	15.10	9.28	7.09	3.99	2.53	1.71	1.30
Eastbound	7,763	12,157	15.12	9.57	7.56	4.54	2.98	2.09	1.57

Note. The average pavement temperature in the westbound and eastbound directions of the section containing the $CaCl_2$ was 68.8 ^oF and 72 ^oF respectively.

Table A.2

Falling Weight Deflectometer data obtained from pavement section containing the untreated RAP base.

Direction	Distance (ft.)	Impact Load (lbs)	Deflections (mils)						
			D_0	D_1	D_2	D_3	D_4	D_5	D_6
Westbound	394	12,279	18.39	12.08	9.34	5.72	4.19	3.19	2.55
Westbound	1,170	12,296	15.49	9.59	7.03	3.92	2.47	1.55	0.95
Westbound	2,210	12,129	19.82	13.68	10.95	6.52	4.27	2.89	2.07
Eastbound	443	12,084	21.20	14.44	11.34	6.43	4.12	2.74	1.97
Eastbound	1,234	12,237	17.28	11.16	8.43	4.39	2.65	1.79	1.31
Eastbound	1,915	12,275	15.06	9.00	7.04	3.91	2.58	1.81	1.35

Note. The average pavement temperature in the westbound and eastbound directions of the section containing the $CaCl_2$ was 70.3 ^oF and 72.3 ^oF respectively.

Table A.3

Falling Weight Deflectometer data obtained from pavement section containing the Portland cement stabilized base.

Direction	Distance (ft.)	Impact Load (lbs)	Deflections (mils)						
			D_0	D_1	D_2	D_3	D_4	D_5	D_6
Westbound	1,036	12,526	9.17	6.58	5.90	4.53	3.31	2.43	1.83
Westbound	2,790	12,433	12.78	9.93	8.80	6.28	4.48	3.18	2.34
Westbound	4,620	12,387	11.87	8.93	7.95	5.75	4.13	3.00	2.23
Westbound	6,465	12,418	12.27	9.29	8.59	6.73	5.10	3.76	2.82
Westbound	8,317	12,352	8.83	6.17	5.62	4.22	3.04	2.15	1.57
Westbound	10,222	12,365	10.76	7.68	6.78	4.61	3.16	2.15	1.57
Westbound	12,015	12,306	8.58	5.82	5.21	3.89	2.68	1.79	1.19
Westbound	13,853	12,376	9.06	6.37	5.74	4.22	2.99	2.13	1.59
Eastbound	1,042	12390	10.10	7.47	6.82	5.17	3.88	2.87	2.20
Eastbound	2,797	12403	9.97	7.04	6.25	4.58	3.23	2.27	1.69
Eastbound	4,616	12254	10.25	7.61	7.04	5.43	4.07	2.98	2.26
Eastbound	6,483	12330	9.08	6.34	5.54	3.75	2.37	1.49	0.93
Eastbound	8,356	12370	11.36	9.09	8.51	6.83	5.29	4.11	3.29
Eastbound	10,191	12382	10.59	8.46	7.85	6.08	4.60	3.2	2.64
Eastbound	12,006	12255	9.83	7.50	6.89	5.41	4.21	3.28	2.71
Eastbound	13,862	12275	13.20	10.35	9.37	7.03	5.19	3.63	2.62

Note. The average pavement temperature in the westbound and eastbound directions of the section containing the $CaCl_2$ was 61.8 ^oF and 60.1 ^oF respectively.

Table A.4

Falling Weight Deflectometer data obtained from pavement section containing the geogrid stabilized base.

Direction	Distance (ft.)	Impact Load (lbs)	Deflections (mils)						
			D_0	D_1	D_2	D_3	D_4	D_5	D_6
Westbound	540	11,999	23.57	15.35	12.10	7.06	4.49	2.88	1.88
Westbound	1,505	11,903	29.29	21.28	17.02	10.24	6.92	4.68	3.27
Westbound	2,500	12,006	24.14	15.96	11.69	6.29	4.14	2.81	1.95
Eastbound	501	12,134	19.88	11.33	8.01	4.33	2.92	2.01	1.49
Eastbound	1,515	11,925	22.90	15.36	11.75	6.58	4.32	3.00	2.12
Eastbound	2,505	12,030	12.75	12.92	10.19	5.46	3.28	2.14	1.53

Note. The average pavement temperature in the westbound and eastbound directions of the section containing the $CaCl_2$ was 66.7 ^oF and 66.3 ^oF respectively.

Table A.5

Falling weight deflectometer data obtained from pavement section containing the bituminous stabilized base.

Direction	Distance (ft.)	Impact Load (lbs)	Deflections (mils)						
			D_0	D_1	D_2	D_3	D_4	D_5	D_6
Westbound	738	12,111	21.34	12.74	9.05	5.05	3.70	2.91	2.34
Westbound	2,290	12,102	17.72	8.42	5.40	2.38	1.45	1.00	0.72
Westbound	3,685	12,114	20.80	12.38	8.95	5.40	3.93	2.97	2.28
Westbound	5,910	12,046	21.21	13.51	10.71	7.18	5.44	4.27	3.46
Eastbound	0	12150	17.32	12.18	9.82	5.92	4.20	3.14	2.53
Eastbound	822	12101	21.22	15.96	12.94	7.74	5.41	4.07	3.29
Eastbound	2,623	12,266	14.56	7.92	5.25	2.16	1.04	0.60	0.42
Eastbound	3,836	12194	17.22	8.84	5.88	2.65	1.35	0.72	0.42

Note. The average pavement temperature in the westbound and eastbound directions of the section containing the $CaCl_2$ was 84.5 ^oF and 68 ^oF respectively.